# International Journal of Analysis and Applications



## Evolution of Radiative Initial Data in Higher-Order Nonlinear Schrödinger Equations: Stability Study

Umar Muhammad Dauda<sup>1,\*</sup>, Diaa S. Metwally<sup>2</sup>, Sani Saleh Musa<sup>3</sup>, Auwal Lawan<sup>1</sup>, H. E. Semary<sup>4</sup>, Mohammed Elgarhy<sup>5</sup>

<sup>1</sup>Department of Mathematics, Faculty of Computing & Mathematical Sciences, Kano University of Science & Technology, Kano, Nigeria

<sup>2</sup>Department of Accounting, Faculty of Business, Imam Mohammad Ibn Saud Islamic University (IMSIU), Riyadh 11432, Saudi Arabia

<sup>3</sup>Department of Mathematics, Jigawa State College of Education & Legal Studies, Jigawa, Nigeria

\*Corresponding author: umarmd2021@gmail.com

**Abstract.** This article presents a comprehensive numerical investigation of the fourth-order Schrödinger equation (FSE), a dispersive partial differential equation characterized by higher-order linear terms and nonlinear interactions for a localized and radiative initial data. Using the Implicit-Explicit (IMEX) splitting method, we address the computational challenges posed by the equation, balancing efficiency and stability for both localized and radiative initial data. We analyze the effects of dispersive parameters ( $\beta$  and  $\gamma$ ) and nonlinear growth parameters ( $\alpha$  and q) on the boundedness of the solutions. A dynamic framework is proposed to track stability using Sobolev norms and energy functionals. The numerical schemes are implemented with Fourier spectral methods for spatial discretization and Runge-Kutta schemes for time evolution. Our results demonstrate the efficacy of the IMEX splitting method in handling stiff dispersive terms while providing insights into parameter sensitivity. In addition, radiative initial data evolves into a decomposed smaller wave-packets.

#### 1. Introduction

1.1. **The fourth order Nonlinear Schrödinger (FNLS) Equations.** The fourth-order Schrödinger equation (FSE) is a nonlinear dispersive partial differential equation that arises in various physical

Received: Jul. 23, 2025.

2020 Mathematics Subject Classification. 35Q55.

*Key words and phrases.* dispersive; nonlinearity; infinitesimal vector field; symmetries; biharmonic; stability; control; singularity; radiative initial data.

ISSN: 2291-8639

<sup>&</sup>lt;sup>4</sup>Department of Mathematics and Statistics, Faculty of Science, Imam Mohammad Ibn Saud Islamic University (IMSIU), Riyadh 11432, Saudi Arabia

<sup>&</sup>lt;sup>5</sup>Department of Basic Sciences, Higher Institute of Administrative Sciences, Belbeis, AlSharkia, Egypt

models, including fluid dynamics, quantum mechanics, and optical systems. Mathematically, it is expressed as:

$$iu_t + \beta u_{xxx} + \gamma u_{xx} + \alpha |u|^q u = 0 \tag{1.1}$$

where u(x,t) is the complex-valued solution, and the parameters  $\beta$ ,  $\gamma$ ,  $\alpha$ , and q characterize the equation's dispersive and nonlinear properties.

This equation poses significant challenges due to the interplay between high-order dispersive terms and nonlinear interactions, which can lead to instability or energy concentration (blow-up) if not properly managed. The primary goal of this work is to address these challenges through efficient numerical methods and rigorous analysis.

One prominent numerical approach for such equations is the IMEX splitting method, which splits the equation into stiff linear and non-stiff nonlinear parts. The linear part is solved implicitly to ensure stability, while the nonlinear part is handled explicitly for computational efficiency. We further analyze the stability and boundedness of solutions using Sobolev norms and energy functionals, providing insights into the role of parameters  $\beta/\gamma$  and  $\alpha/q$ .

The Nonlinear Schrödinger (NLS) equation and its extensions have been extensively studied in the context of dispersive and nonlinear systems. Classical studies, such as [18], explored the theoretical properties of dispersive equations, focusing on existence, uniqueness, and blow-up phenomena. Two dimensional version of the NLS equation such as Davey-Stewartson Systems are studied in greater detail, some of the recent results are found in Joerg et. al. [10].

Higher-order Schrödinger equations, including the Fourth Order Nonlinear Schrödinger (FNLS) equation, have gained attention for their applications in quantum mechanics and wave propagation. As we are interested in equation that of fourth order, such as the biharmonic equations, some of the recent results are found in the literature [16] where dispersive and nonlinearity effects were studied. Numerical methods for such equations include spectral methods [20], time-splitting methods [13], and Runge-Kutta schemes [4]. The IMEX splitting method, analyzed in [3], has proven effective for equations with stiff linear operators, balancing stability and computational cost. For the spectral methods of implementation for some of these dispersive equations see [20].

For the existing results on similar kind of nonlinear dispersive equations, see [5]. In the work by Capistrano-Filho, a higher-order generalized kind of KdV is studied using rigorous analysis approach that involves some dispersive estimates. A controllability study of the KdV-equation on a bounded domain is carried out by [6]. Similar studied were done on the extended KdV-type of equation [7] [8].

For the theoretical understanding of these kind of equations on different kind of domain and boundaries read Kato (2012) [12], and some existing local and global analysis of some nonlinear related Schrödinger equations (Tao, 2006 [19]). On the control and stability studies of other kind of dispersive equations, read [21], [22] and Zhao (2018). Another study of a modified dispersive equation is carried out on energy decay of the solution on a bounded domain [1].

In addition, Sobolev embedding theorems and energy conservation laws have been used to establish the boundedness of solutions in nonlinear PDEs [9]. For more similar studies on different kind of equation see [7] and [8] using Sobolev Spaces. These tools are essential for understanding the dynamics of the NLFS equaiton and its parameter sensitivity.

#### 2. Properties of the FNSE

Knowing fully the geometric and algebraic properties of the equation will help a lot in understanding the properties of the equation and its solutions. The equation (1.1), like the classical nonlinear Schrödinger equation, has its mass and energy functionals defined as

$$M[u(t)] = \int_{\mathbb{R}} |u|^2 dx = ||u||_{L_2}^2$$
 (2.1)

$$E[u(t)] = \int_{\mathbb{R}} \left( \gamma |u_x|^2 - \beta |u_{xx}|^2 - \frac{2\alpha}{q+2} |u|^{q+2} \right) dx, \quad q \ge 2.$$
 (2.2)

Consequent to this, the equation (1.1) like the classical NLS equation, has, associated to it, some invariants. Based on the Noether's theorem we can have the following symmetries:

(1) **Translation Symmetry**: The equation is invariant under spatial and temporal translations:

$$u(x,t) \mapsto u(x+x_0,t+t_0).$$

(2) Scaling Symmetry:

For specific choices of  $\beta$ ,  $\gamma$ ,  $\alpha$ , the equation is invariant under the scaling transformation:

$$u(x,t) \mapsto \lambda^{-2/q} u(\lambda x, \lambda^4 t).$$

(3) Phase Symmetry:

The equation remains invariant under a global phase transformation:

$$u(x,t)\mapsto e^{i\theta}u(x,t),$$

where  $\theta \in \mathbb{R}$ .

(4) Pseudo conformal Transformation:

$$u(x,t) \to \frac{e^{i|x-x_0|^2/4\beta(t-t_0)}}{|t-t_0|^{1/2}}u\left(\frac{x-x_0}{t-t_0}, -\frac{1}{t-t_0}\right),$$

where  $|t-t_0|^{-1/2}$  is a scaling factor that to preserve the  $L^2$ -norm,  $e^{i|x-x_0|^2/4\beta(t-t_0)}$  is a phase factor, as in the phase-transformation, to compensate for the spatial transformation while  $\frac{x-x_0}{t-t_0}$ ,  $-\frac{1}{t-t_0}$  are meant for the inversion, respectively, in space and time.

Proof of some of these symmetries are provided as follows:

- (1) Translation symmetries
  - Time translation:  $t \to t + t_0$  for  $t' = t + t_0$ , x' = x, u'(x',t') = u(x,t) under the transformation,  $u'(x',t') = u(x,t+t_0)$ , so we have

$$\frac{\partial u'}{\partial t} = \frac{\partial u}{\partial t}, \quad u'_{xxxx} = u_{xxxx}, \quad u'_{xx} = u_{xx}$$

Thus,  $iu'_t + \beta u'_{xxxx} + \gamma u'_{xx} + \alpha |u'|^q u' = 0$ , Since each term remains invariant.

• Space translation  $(x \rightarrow x + x_0)$ 

For a space translation, shift  $x \to x + x_0$ ,  $x' = x + x_0$ , t' = t,  $u'(x', t') = u(x + x_0, t)$ .

The spatial derivatives remain unchanged:

$$\frac{\partial u'}{\partial x'} = \frac{\partial u}{\partial x}, \quad u'_{xxxx} = u_{xxxx}, \quad u'_{xx} = u_{xx}$$

and the time derivative

$$\frac{\partial u}{\partial t'} = \frac{\partial u}{\partial t}$$

Therefore  $iu'_t + \beta u'_{xxxx} + \gamma u'_{xx} + \alpha |u'|^q u' = 0$ .

(2) Phase symmetry:

$$u'(x',t') = u(x,t)e^{i\theta}$$
  $x' = x,t' = t$ 

For phase shift by  $\theta$ , we modify the wave function as  $u(x,t) \to u(x,t)e^{i\theta}$  For the time derivative

$$\frac{\partial u'}{\partial t'} = u_t' = u_t e^{i\theta}$$

$$u_x' = u_x e^{i\theta}$$
,  $u_{xx}' = u_{xx} e^{i\theta}$ ,  $u_{xxxx}' = u_{xxxx} e^{i\theta}$ 

Considering the non linear part

$$|u|^q \to |u'(x',t')|^q = |u(x,t)e^{i\theta}|^q = |u(x,t)|^q |e^{i\theta}|^q = |u(x,t)|^q$$

then 
$$|u'(x; t')|^q u'(x', t') = |u(x, t)|^q u(x, t) e^{i\theta}$$
.

Substituting into the main equation (1.1) we have

$$iu'_t + \beta u'_{xxxx} + \gamma u'_{xx} + \alpha |u'|^q u' = e^{i\theta} (iu_t + \beta u_{xxxx} + \gamma u_{xx} + \alpha |u|^q u) = 0.$$

(3) Galilean symmetry:

$$x' = x - ct$$
,  $u'(x', t') = u(x, t)e^{i(cx - \frac{c^2t}{2})}$ 

In a Galilean transformation, we move to a reference frame moving with velocity c. This introduces a phase form in the wave function. There, we have

$$u'_{t} = \frac{\partial u'}{\partial t'} = \frac{\partial (u(x,t)e^{cx - \frac{c^{2}t}{2}})}{\partial t} = \left(u_{t} + icu_{x} - \frac{ic^{2}}{2}u\right)e^{i(cx - \frac{c^{2}t}{2})}$$

$$u'_{x} = \frac{\partial u'}{\partial x'} = \frac{\partial}{\partial x}\left(u(x,t)e^{i(cx - \frac{c^{2}t}{2})}\right) = \left(u_{x} + iuc\right)e^{i(cx - \frac{c^{2}t}{2})},$$

$$u'_{xx} = (u_{xx} + 2icu_{x} - uc^{2})e^{i(cx - \frac{c^{2}t}{2})},$$

$$u'_{xxx} = (u_{xxx} + 3iu_{xx}c - 3c^{2}u_{x} - iuc^{3})e^{i(cx - \frac{c^{2}t}{2})},$$

$$u'_{xxxx} = (u_{xxxx} + 4icu_{xxx} - 6c^{2}u_{xx} - 4ic^{3}u_{x} + uc^{4})e^{i(cx - \frac{c^{2}t}{2})}.$$

Similarly, for the nonlinear part:

$$|u'(x',t')|^q = |u(x,t)e^{i(cx-\frac{c^2t}{2})}|^q = |u(x,t)|^q$$

since 
$$|e^{i(cx-\frac{c^2t}{2})}|^2 = 1$$

Again, substituting back into the main equation one gets:

$$iu'_{t} + \beta u'_{xxxx} + \gamma u'_{xx} + \alpha |u'|^{2}u' = e^{i(cx - \frac{c^{2}t}{2})} \left[ \left( iu_{t} + i^{2}cu_{x} - i^{2}\frac{c^{2}u}{2} \right) + \beta (u_{xxxx} + 4icu_{xxx} - 6c^{2}u_{xx} - 4ic^{3}u_{x} + uc^{4}) + \gamma (u_{xx} + 2icu_{x} - uc^{2}) + \alpha |u|^{q}u \right]$$

$$= e^{i(cx - \frac{c^{2}t}{2})} \left[ \left( \frac{c^{2}u}{2} - cu_{x} \right) + \beta c^{2}(uc^{2} - 6u_{xx}) - \gamma c^{2}u + i(4c\beta u_{xxx} - 4c^{3}u_{x} + 2\gamma cu_{x}) \right]$$

This implies that the equation stays invariant provided that the following conditions

$$\left(\frac{c^2u}{2} - cu_x\right) + \beta c^2(uc^2 - 6u_{xx}) - \gamma c^2u = 0,$$

$$4c\beta u_{xxx} - 4c^3u_x + 2\gamma cu_x = 0$$

hold.

2.1. **Local Gauge Transform and Invariance.** Here we investigate the invariance property of the main equation (1.1) under local gauge transformation. It turns out that the global one holds (phase transform).

The local Guage transform modifies the solution u(x, t) as:

$$u(x,t) \mapsto u'(x,t) = u(x,t)e^{i\phi(x,t)},$$

where  $\phi(x,t)$  is a smooth real-valued function. Substituting u'(x,t) into the FSE, we obtain the transformed equation:

$$iu'_{t} + \beta u'_{xxxx} + \gamma u'_{xx} + \alpha |u'|^{q}u' = (\beta \phi_{x}^{2} - \phi_{t} - \gamma \phi_{x}^{2} - 4\beta \phi_{xxx}\phi_{x} - 3\beta \phi_{xx}^{2})u - 6\beta u_{xx}\phi_{x}^{2}$$

$$- 12\beta u_{x}\phi_{xx}\phi_{x} + u|u|^{q} + \beta u_{xxxx} + \gamma u_{xx} + i \left[ 4\beta u_{xxx}\phi_{x} + 6\beta u_{xx}\phi_{xx} + \gamma \phi_{xx} + 4\beta u_{x}\phi_{xxx} - 4\beta u_{x}\phi_{x}^{3} - 6\beta u\phi_{x}^{2}\phi_{xx} + 2\gamma u_{x}\phi_{x} + u_{t} \right]$$

$$= ([\beta - \gamma]\phi_{x}^{2} - \phi_{t} - 4\beta \phi_{xxx}\phi_{x} - 3\beta \phi_{xx}^{2})u - 6\beta u_{xx}\phi_{x}^{2} - 12\beta u_{x}\phi_{xx}\phi_{x}$$

$$+ i \left[ (4\beta u_{xxx} - 4\beta u_{x}\phi_{x}^{2} - 6\beta u\phi_{x}\phi_{xx} + 2\gamma u_{x})\phi_{x} + [6\beta u_{xx} + \gamma]\phi_{xx} + 4\beta u_{x}\phi_{xxx} + \beta u\phi_{xxxx} \right]$$

$$(2.3)$$

The equation remains invariant under the gauge transformation provided that:

$$([\beta - \gamma]\phi_x^2 - \phi_t - 4\beta\phi_{xxx}\phi_x - 3\beta\phi_{xx}^2)u - 6\beta u_{xx}\phi_x^2 - 12\beta u_x\phi_{xx}\phi_x = 0;$$

$$(4\beta u_{xxx} - 4\beta u_x\phi_x^2 - 6\beta u\phi_x\phi_{xx} + 2\gamma u_x)\phi_x + [6\beta u_{xx} + \gamma]\phi_{xx} + 4\beta u_x\phi_{xxx} + \beta u\phi_{xxxx} = 0.$$

This invariance condition restricts the choice of  $\phi(x,t)$ , ensuring the transformation does not alter the dynamics. More relaxing conditions may leads to the promising new solutions.

2.2. **Dispersive Nature of The equation.** The dispersive nature of the FSE is determined by its dispersion relation. Assuming  $u(x,t) = e^{i(kx-\omega t)}$ , substituting into the linearized equation:

$$iu_t + \beta u_{xxxx} + \gamma u_{xx} = 0,$$

yields the dispersion relation:

$$\omega(k) = \gamma k^2 - \beta k^4.$$

The group velocity,  $v_g = \frac{d\omega}{dk}$ , is:

$$v_{g}(k) = 2\gamma k - 4\beta k^{3}.$$

while the phase velocity  $v_p = \omega/k = \gamma k - \beta k^3 \neq v_g$ . The dispersion relation is shown in Fig.

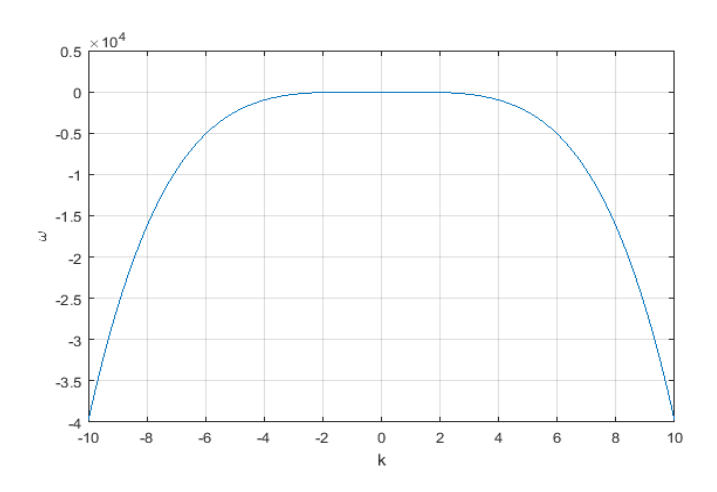


Figure 1. The dispersion relation  $\omega(k)$  for the linearised form of the nonlinear 4th order equation.

For  $\beta > 0$ , the fourth-order dispersion term dominates for large k, leading to highly dispersive behavior. The balance between  $\beta$  and  $\gamma$  determines the relative contributions of higher- and lower-order dispersive effects. This dispersive nature influences wave propagation and stability, making parameter tracking critical for numerical simulations.

2.3. **Derivation via the Euler-Lagrange Equation.** The Euler-Lagrange equation for a complex-valued field is:

$$\frac{\partial}{\partial t} \left( \frac{\partial \mathcal{L}}{\partial u_t^*} \right) + \frac{\partial}{\partial x} \left( \frac{\partial \mathcal{L}}{\partial (\partial_x u^*)} \right) - \frac{\partial^2}{\partial x^2} \left( \frac{\partial \mathcal{L}}{\partial (\partial_x^2 u^*)} \right) - \frac{\partial \mathcal{L}}{\partial u^*} = 0.$$

Firstly by computing the partial derivatives of  $\mathcal{L}$  as found according to the Euler's Lagrange equation, we found:

$$\frac{\partial \mathcal{L}}{\partial u_t^*} = -\frac{i}{2}u, \qquad \frac{\partial \mathcal{L}}{\partial (\partial_x u^*)} = -\gamma \partial_x u,$$
$$\frac{\partial \mathcal{L}}{\partial (\partial_x^2 u^*)} = \beta \partial_x^2 u, \quad \frac{\partial \mathcal{L}}{\partial u^*} = \frac{i}{2}u_t - \frac{\alpha}{2}|u|^q u.$$

Substituting into Euler-Lagrange Equation, we obtain:

$$iu_t + \beta \partial_x^4 u + \gamma \partial_x^2 u + \alpha |u|^q u = 0,$$

which recovers the original fourth-order Schrödinger equation.

3. Methodology: Control Analysis

3.1. **Splitting Technique.** We decompose the equation into linear and nonlinear parts:

$$iu_t + \mathcal{L}_4 u = 0, \quad iu_t + \alpha |u|^q u = 0.$$
 (3.1)

The linear evolution equation is solved using a spectral method, which efficiently handles the dispersive operator:

$$\mathcal{L}_4 = \beta \partial_x^4 + \gamma \partial_x^2 \tag{3.2}$$

We define

$$\hat{u}(t,k) = \mathcal{F}[u](t,k) = \int_{-\infty}^{\infty} e^{-ikx} u(t,x) dx, \qquad \mathcal{F}^{-1}[u](t,x) = \int_{-\infty}^{\infty} e^{ikx} \hat{u}(t,k) dk = u(t,x),$$

as the Fourier Transform  $\mathcal{F}$  of the function u(t,x) in x and its inverse Fourier transform  $\mathcal{F}^{-1}$ .

Applying the Fourier Transformation to the linear part equation we write:

$$i\hat{u}_t = i\widehat{\mathcal{L}_4 u} = i\hat{\mathcal{L}}_4 \hat{u}; \tag{3.3}$$

where

$$\hat{\mathcal{L}}_4 = \beta k^4 - \gamma k^2.$$

To obtain the solution of the equation, we apply the IMEX (Implicit-Explicit) splitting method. It is a time integration technique that splits the terms of the partial differential equation (PDE) into *linear (stiff)* and *nonlinear (non-stiff)* components. It is particularly effective for higher dispersive equations such as the underlying nonlinear 4th order nonlinear Schrödinger equation. The description of the method is highlighted as follows.

- 3.2. **Description of the IMEX splitting.** Here we describe how the IMEX splitting technique is applied to our dispersive equation.
  - (1) **Splitting the Equation**: The equation is split into two parts:
    - Linear Component (stiff):

$$iu_t + \mathcal{L}_4 u = 0.$$

• Nonlinear Component (non-stiff):

$$iu_t + \alpha |u|^q u = 0.$$

The IMEX method treats the *linear component* implicitly for stability and the *nonlinear component* explicitly for computational efficiency.

## (2) Time-Stepping Scheme

Let  $u^n$  be the solution at time  $t = n\Delta t$ , where  $\Delta t$  is the time step size. The IMEX splitting method advances the solution from  $u^n$  to  $u^{n+1}$  in two steps:

• **Step 1**: Linear Evolution (Implicit) Solve the linear part implicitly:

$$u^{n+1/2} = e^{-i\mathcal{L}_4\Delta t}u^n,$$

where  $e^{-i\mathcal{L}_4\Delta t}$  is the matrix exponential operator, typically computed in Fourier space for efficiency.

• **Step 2**: Nonlinear Evolution (Explicit) Evolve the nonlinear part explicitly:

$$u^{n+1} = u^{n+1/2} - i\Delta t \alpha |u^{n+1/2}|^q u^{n+1/2}.$$

## (3) Applying the Method step-by-step:

- Initialize:
  - Define the initial condition  $u_0(x)$ , and parameters  $\beta$ ,  $\gamma$ ,  $\alpha$ , and q.
  - Set up the spatial grid and Fourier transform operators.
- Linear Evolution:
  - Use the Fourier transform to diagonalize the linear operator  $\mathcal{L}_4$ .
  - Compute the matrix exponential  $e^{-i\mathcal{L}_4\Delta t}$  efficiently in Fourier space.
- Nonlinear Evolution:
  - Compute the nonlinear term  $\alpha |u|^q u$  explicitly in physical space.
- Advance Time: Combine the linear and nonlinear components to update the solution.

## (4) Stability and Accuracy

For stability,

- Implicit Linear Step:
  - The stiff linear operator  $\mathcal{L}_4$  is treated implicitly, ensuring numerical stability for large time steps.

For accuracy,

## • Explicit Nonlinear Step:

- The nonlinear term is non-stiff and is evaluated explicitly, avoiding expensive implicit solvers.

The accuracy of the approach from the first order splitting leads to the order one accuracy in time. One achieves higher-order-accuracy by applying this method of *Strang splitting*, where the sequence is modified as:

$$u^{n+1} = e^{-i\mathcal{L}_4 \frac{\Delta t}{2}} \left( u^n - i\Delta t \alpha |u^n|^q u^n \right) e^{-i\mathcal{L}_4 \frac{\Delta t}{2}}.$$

This improves the accuracy to second-order in time.

One of the advantages of this method (IMEX splitting) for this problem include the *computational efficiency* which is achieve due to diagonalization in the Fourier space, while the implicit linear

step avoid expensive matrix inversions. The stability is another advantage which is attained by handling the stiffness from the linear dispersion operator  $\mathcal{L}_4$  efficiently. It can further be adapted to higher schemes such as Strang splitting.

- 3.3. **Algorithms & Stability Tracking.** Below are two algorithms that address the choice of the nonlinearity where stability is guaranteed:
- 3.4. **Tracking Stability of Dispersive Effects** ( $\beta/\gamma$ ). This algorithm evaluates and tracks the impact of dispersive terms on the solution stability using the Sobolev embedding theorem. The Sobolev  $H^2$ -norm is bounded to analyze stability.

## **Algorithm Description**

• Define the fourth-order Schrödinger equation:

$$iu_t + \beta u_{xxxx} + \gamma u_{xx} + \alpha |u|^q u = 0$$

- Decompose the equation into linear and nonlinear parts:
  - $-\mathcal{L}_4 u = \beta \partial_r^4 u + \gamma \partial_r^2 u$
  - Nonlinear term:  $\alpha |u|^q u$ .
- Compute the Sobolev embedding bounds for the linear operator:

$$||u||_{L^\infty} \leq C||u||_{H^2}.$$

The stability is achieved if the

$$\frac{\|u\|_{H^2}}{\|u_0\|_{H^2}} < \infty \qquad \forall t$$

That's the quantity remains bounded for all time *t*, where

$$||u||_{H^2}^2 := ||u||_{L^2(\mathbb{R})}^2 + ||\nabla u||_{L^2(\mathbb{R})}^2 + ||\nabla^2 u||_{L^2(\mathbb{R})}^2, \qquad ||u||_{L^2(\mathbb{R})}^2 := \int_{\mathbb{R}} |u|^2 dx.$$

- Solve the linear evolution using a spectral method (efficient for dispersive operators).
- 3.5. **Controlling Nonlinear Growth** ( $\alpha/q$ ). This algorithm monitors the nonlinear effects using energy functionals and Sobolev bounds, ensuring that the growth of the nonlinear term  $|u|^q$  is controlled.

## **Algorithm Description**

- Use the define energy functional (2.2)
- Track the energy conservation:

$$\frac{dE[u]}{dt} = 0.$$

• Use the Sobolev embedding to control  $|u|^q$  via:

$$||u||_{L^{\infty}}^{q} \le C||u||_{H^{2}}^{q}.$$

• Solve the nonlinear evolution iteratively using the Duhamel principle:

$$u(t) = e^{i\hat{\mathcal{L}}_4 t} u_0 - i \int_0^t e^{i\hat{\mathcal{L}}_4 (t-s)} \alpha |u|^q u \, ds.$$

• Monitor  $||u||_{H^2}$  and ensure it remains bounded.

#### 4. Numerical Simulation

Here we provide the simulation of the results obtained by using different choice of our parameters. All the simulated results are generated based on the choice of Schwartzian initial data.

• Case I. Taking initial data  $u_0(x) = \operatorname{sech}^2(x-1)$  and  $\alpha = 1, \beta = 0.1, q = 2$  and  $\gamma = 2$ , the solution and the mass and energy conservations of u(t,x) is shown in the Fig. 2 as follows.

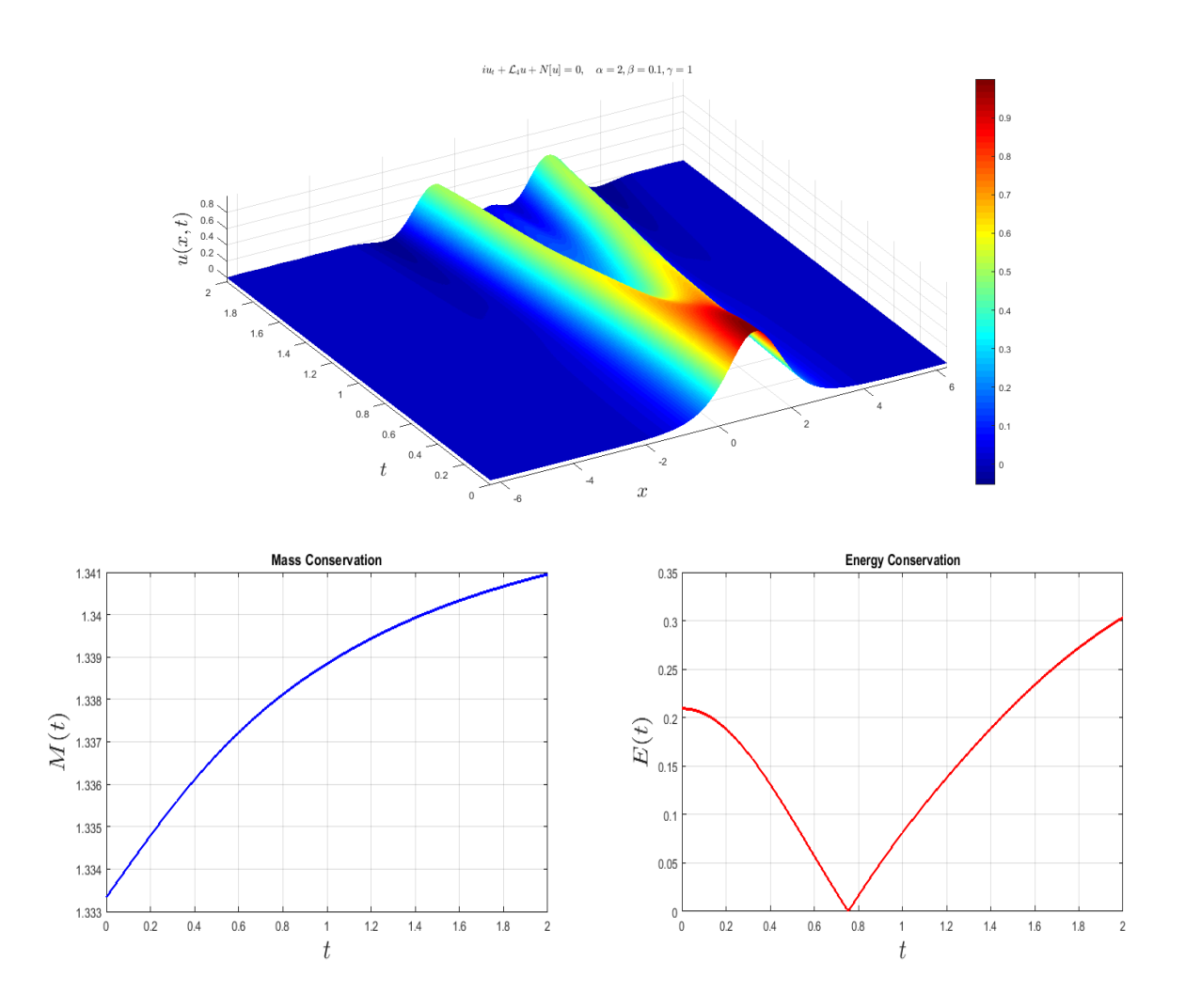


Figure 2. (top) Numerical solution u(t,x) of the equation (1.1) for  $\alpha=1,\beta=0.1,q=2$  and  $\gamma=2$  with  $u_0(x)=\mathrm{sech}^2(x-1)$ . (Bottom) Corresponding evolution of mass and energy over time t.

In this case the biharmonic behaviour is noticed as in the case of classical dispersive beam equation type.

• Case II. The effect of higher nonlinearity and lower dispersion is observed in this case where  $\alpha = 1, \beta = 0.1, q = 2$  and  $\gamma = 2$  using the same type of initial data shown in Fig. 3.

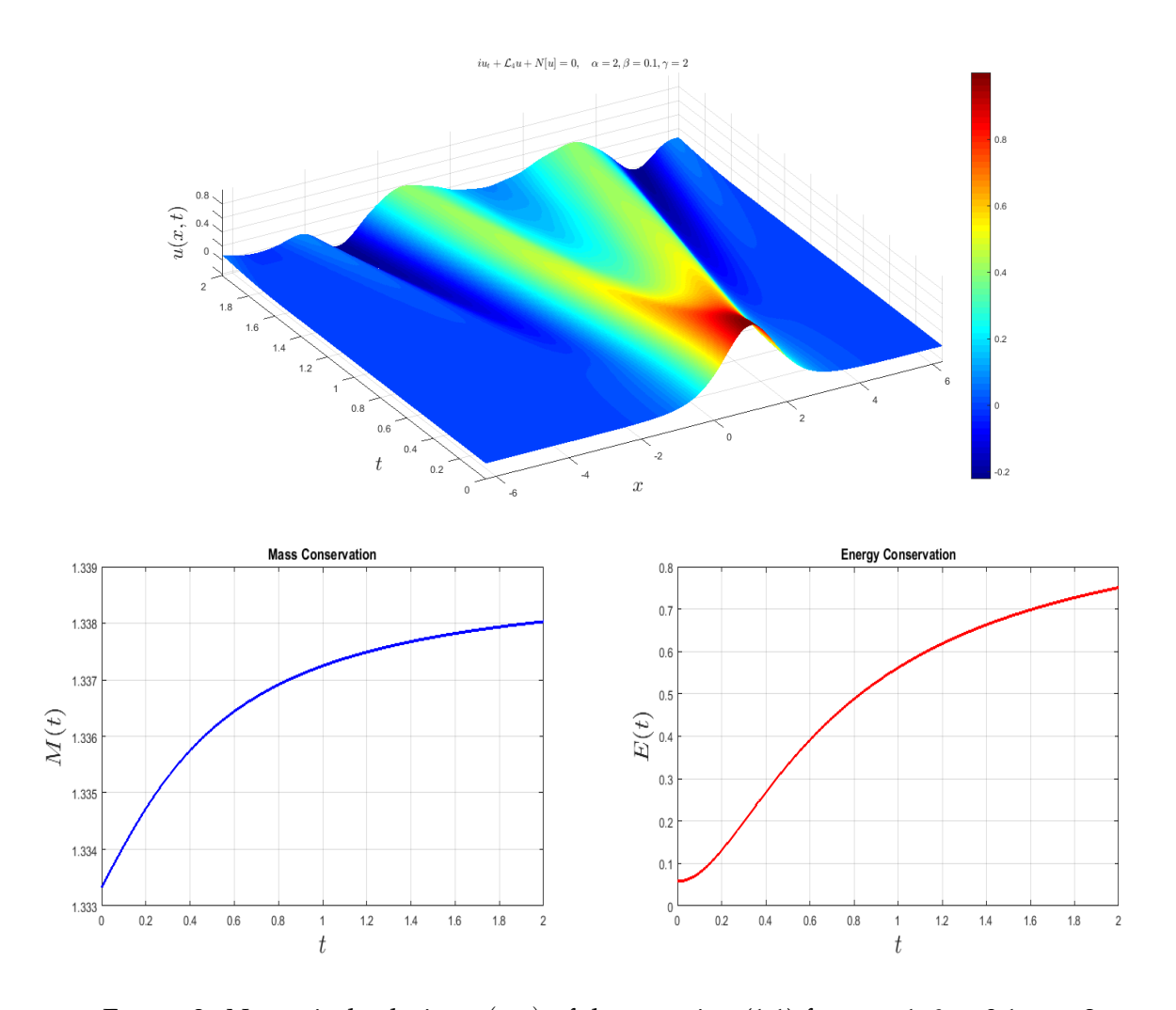


Figure 3. Numerical solution u(t,x) of the equation (1.1) for  $\alpha = 1, \beta = 0.1, q = 2$  and  $\gamma = 2$ .

The mass and the energy conservations show significant variation in comparison with the result shown in Fig. 2.

• Case III. Here the dispersive effect is varied significantly and exponential nonlinearity q is assumed to have larger value. With  $\alpha = 2$ ,  $\beta = 1$ , q = 4 and  $\gamma = 2$ , the result shows an anticipated behaviour. It is expected that stronger nonlinear could have the tendency to alter the dispersion variation by overtaking it, see the behaviour in Fig. 4.

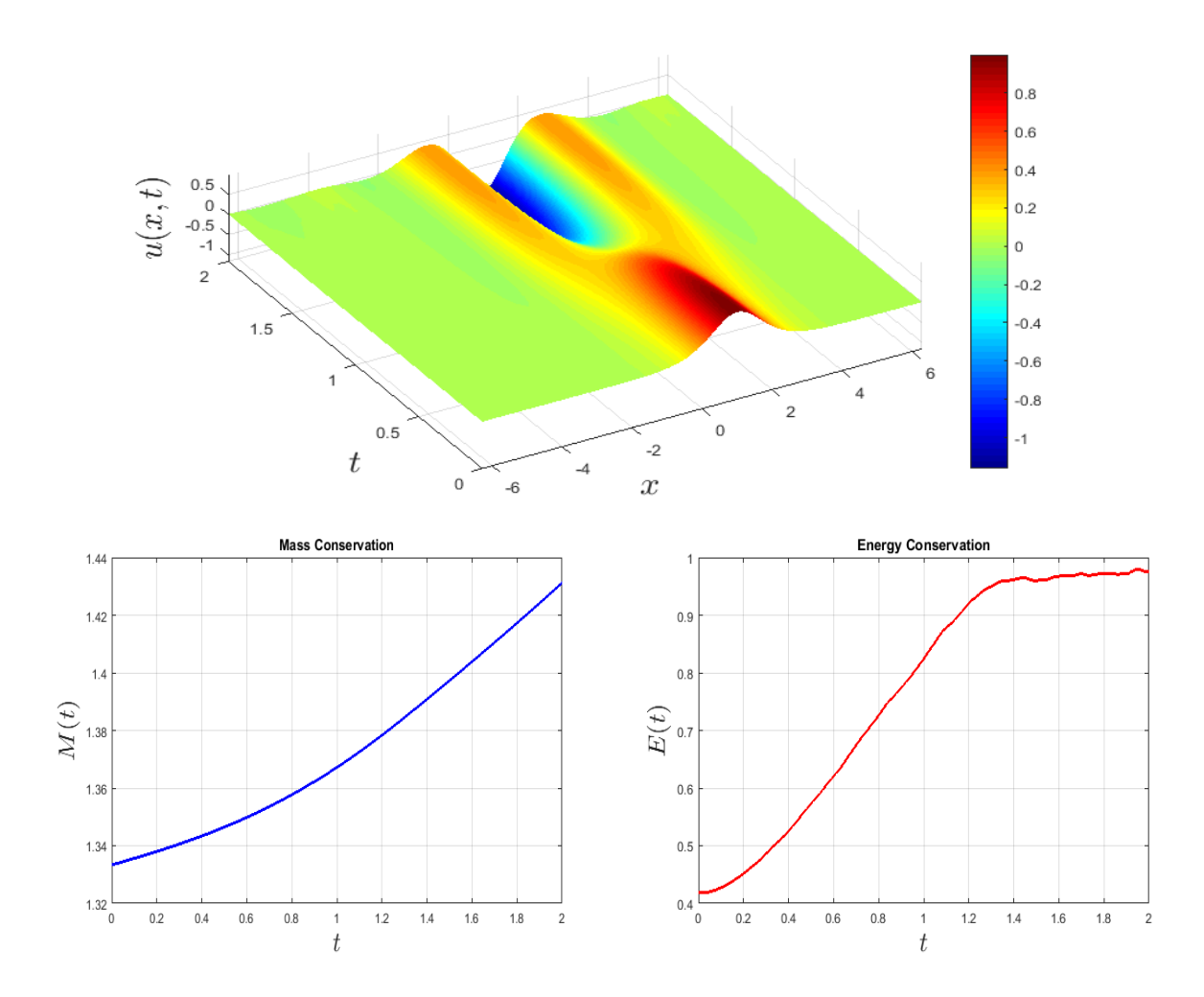


Figure 4. Numerical solution |u(t,x)| of the equation (1.1) for  $\alpha=2,\beta=1,q=4$  and  $\gamma=2$ .

Through out the simulated results, the evolution of the mass and energy functions indicated that there are slight variations as they evolve, however, as it is expected the system is conserved as long as none of the dispersion or nonlinearity effect overtake the other. Thus, when these results are simulated for a long time, the conservation can be guaranteed. However, when we attempt to do that, the stability of the method is compromised since we are using numerical approach, rounding errors tend to accumulate thereby affecting its accuracy. Therefore, for these reasons, we intend to track the dispersive effects as well the nonlinearity effects via the use of  $L_2$  and  $H^2$ -norms of the solution to study the stability of the underlying nonlinear dispersive equation. This is recommended by the Sobolev embedding theorem via the Duhamel formulation (7.6) of the main equation. This is shown in a section on the control analysis.

#### 5. Results and Discussion: Control Analysis

The IMEX splitting method demonstrates stability and efficiency in solving the main equation by dynamically varying the parameters  $\beta/\gamma$  and  $\alpha/q$ . Here we analyse the the stability of the equation based on the choice of parameters  $\alpha, \beta, \gamma, q$ .

- 5.1. **Nonlinearity effect.** For the nonlinearity effect, the time t, mass M(t), energy E(t) and the relative energy E(t)/E(0) are computed. We track the value of the energy and its relative variations over time t. The result is shown while the nonlinearity parameters  $\alpha$  and q vary, the dispersive parameters are fixed. Here, we fixed  $\gamma = 1$  and  $\beta = 0.1$  (small dispersion) and vary the nonlinearity related parameters:  $\alpha$  and q over the intervals  $\alpha$ : [0.5, 1, 2, 4] and  $\gamma$ : [2, 4, 6, 8]:
  - Case I With fixed  $\alpha = 0.5$  and q = 2, or  $\alpha/q = 0.25$  but with small dispersion coefficient  $\beta = 0.1$ , we obtain the evolution of the mass and energy as shown in the table below:

```
Controlling nonlinear Growth for alpha =0.50, q = 2.00, alpha/q = 0.2500
Time Mass Energy Rel.
0.0100 1.3334 0.0193 1.0011
                                                       1.8000 1.3353 0.2400 12.4355
0.0200 1.3334 0.0194 1.0043
                                                       1.8100 1.3353 0.2410 12.4843
0.0300 1.3334 0.0195 1.0096
                                                       1.8200 1.3353 0.2419 12.5327
0.0400 1.3334 0.0196 1.0171
                                                       1.8300 1.3353 0.2428 12.5807
0.0500 1.3334 0.0198 1.0267
                                                       1.8400 1.3353 0.2437 12.6284
0.0600 1.3334 0.0200 1.0383
                                                       1.8500 1.3353 0.2447 12.6758
0.0700 1.3335 0.0203 1.0521
                                                       1.8600 1.3353 0.2456 12.7229
0.0800 1.3335 0.0206 1.0679
                                                       1.8700 1.3354 0.2465 12.7696
0.0900 1.3335 0.0210 1.0858
                                                       1.8800 1.3354 0.2474 12.8159
                                                       1.8900 1.3354 0.2483 12.8620
0.1000 1.3335 0.0213 1.1058
                                                       1.9000 1.3354 0.2491 12.9076
0.1100 1.3335 0.0218 1.1278
                                                       1.9100 1.3354 0.2500 12.9530
0.1200 1.3336 0.0222 1.1519
                                                       1.9200 1.3354 0.2509 12.9980
0.1300 1.3336 0.0227 1.1780
                                                       1.9300 1.3354 0.2517 13.0427
0.1400 1.3336 0.0233 1.2060
                                                       1.9400 1.3354 0.2526 13.0870
0.1500 1.3336 0.0239 1.2361
                                                       1.9500 1.3354 0.2534 13.1310
0.1600 1.3336 0.0245 1.2681
                                                       1.9600 1.3354 0.2543 13.1746
0.1700 1.3336 0.0251 1.3020
                                                       1.9700 1.3354 0.2551 13.2180
0.1800 1.3337 0.0258 1.3379
                                                       1.9800 1.3354 0.2560 13.2610
0.1900 1.3337 0.0266 1.3756
                                                       1.9900 1.3354 0.2568 13.3037
0.2000 1.3337 0.0273 1.4152
                                                       2.0000 1.3354 0.2576 13.3460
```

Figure 5. Table showing the variation of the mass M(t), energy E(t) and the relative energy E(t)/E(0) over time at  $\alpha = 1/2$ , q = 2 for  $\gamma = 1$ ,  $\beta = 0.1$ .

The result shows less significant variation in the mass and energy evolutions.

• Case II For  $\alpha = 0.5$  and q = 4, we have the following results:

```
Controlling nonlinear Growth for alpha =0.50, q =4.00, alpha/q = 0.1250 1.8000 1.3354 0.3757 1.1000
                                                         1.8100 1.3354 0.3758 1.1003
Time Mass
           Energy Rel.
                                                         1.8200 1.3354 0.3759 1.1005
0.0100 1.3354 0.3419 1.0012
                                                         1.8300 1.3354 0.3759 1.1007
0.0200 1.3354 0.3423 1.0023
0.0300 1.3354 0.3427 1.0034
                                                         1.8400 1.3354 0.3760 1.1010
0.0400 1.3354 0.3431 1.0045
                                                        1.8500 1.3354 0.3761 1.1012
0.0500 1.3354 0.3435 1.0056
                                                        1.8600 1.3354 0.3762 1.1015
0.0600 1.3354 0.3438 1.0067
                                                         1.8700 1.3354 0.3763 1.1017
0.0700 1.3354 0.3442 1.0078
                                                         1.8800
                                                                 1.3354 0.3764 1.1020
0.0800 1.3354 0.3446 1.0088
                                                         1.8900
                                                                 1.3354 0.3764 1.1022
0.0900 1.3354 0.3449 1.0099
                                                         1.9000 1.3354 0.3765 1.1025
0.1000 1.3354 0.3453 1.0109
                                                         1.9100 1.3354 0.3766 1.1027
0.1100 1.3354 0.3456 1.0119
                                                        1.9200 1.3354 0.3767 1.1029
0.1200 1.3354 0.3459 1.0129
                                                        1.9300 1.3354 0.3768 1.1032
0.1300 1.3354 0.3463 1.0139
                                                        1.9400 1.3354 0.3769 1.1034
0.1400 1.3354 0.3466 1.0149
                                                        1.9500 1.3354 0.3769 1.1037
0.1500 1.3354 0.3470 1.0159
                                                        1.9600 1.3354 0.3770 1.1039
0.1600 1.3354 0.3473 1.0168
                                                        1.9700 1.3354 0.3771 1.1041
0.1700 1.3354 0.3476 1.0178
                                                        1.9800 1.3354 0.3772 1.1044
0.1800 1.3354 0.3479 1.0187
                                                        1.9900
                                                                 1.3354 0.3773 1.1046
0.1900 1.3354 0.3482 1.0196
                                                         2.0000 1.3354 0.3773 1.1048
0.2000 1.3354 0.3485 1.0205
```

Figure 6. Table showing the variation of the mass M(t), energy E(t) and the relative energy E(t)/E(0) over time at  $\alpha = 1/2$ , q = 2 but  $\gamma = 1$ ,  $\beta = 0.1$ .

One notices some variations in the  $H^2$ -norms even-though the mass and the energy evolution appear somewhat stable, Fig. 6. This is noted from the ratio of the  $H^2$ -norm. The behaviour occurs due to the increased in the non-linearity exponent q for small dispersion coefficient  $\beta$ .

• **Case III:** As we notice what increase in *q* could result to, let us vary  $\alpha$ . For  $\alpha = 1$  and q = 6, we have:

```
Controlling nonlinear Growth for alpha =0.50, q =6.00, alpha/q = 0.0833
                                                        1.8100 1.3354 0.3860 1.0044
Time Mass Energy Rel.
                                                       1.8200 1.3354 0.3860 1.0044
0.0100 1.3354 0.3844 1.0000
                                                       1.8300 1.3354 0.3860 1.0044
0.0200 1.3354 0.3844 1.0001
                                                       1.8400 1.3354 0.3860 1.0044
0.0300 1.3354 0.3844 1.0001
                                                       1.8500 1.3354 0.3860 1.0044
0.0400 1.3354 0.3844 1.0002
                                                       1.8600 1.3354 0.3860 1.0044
0.0500 1.3354 0.3844 1.0002
0.0600 1.3354 0.3845 1.0003
                                                       1.8700 1.3354 0.3860 1.0044
0.0700 1.3354 0.3845 1.0003
                                                       1.8800 1.3354 0.3860 1.0044
 0.0800 1.3354 0.3845 1.0004
                                                       1.8900 1.3354 0.3860 1.0044
0.0900 1.3354 0.3845 1.0004
                                                        1.9000
                                                                1.3354 0.3861 1.0045
0.1000 1.3354 0.3845 1.0005
                                                       1.9100 1.3354 0.3861 1.0045
0.1100 1.3354 0.3845 1.0005
                                                       1.9200 1.3354 0.3861 1.0045
0.1200 1.3354 0.3846 1.0006
                                                       1.9300 1.3354 0.3861 1.0045
0.1300 1.3354 0.3846 1.0006
                                                       1.9400 1.3354 0.3861 1.0045
0.1400 1.3354 0.3846 1.0007
                                                       1.9500 1.3354 0.3861 1.0045
 0.1500 1.3354 0.3846 1.0007
                                                       1.9600 1.3354 0.3861 1.0045
0.1600 1.3354 0.3846 1.0008
                                                       1.9700 1.3354 0.3861 1.0045
 0.1700 1.3354 0.3846 1.0008
                                                       1.9800 1.3354 0.3861 1.0045
 0.1800 1.3354 0.3847 1.0008
                                                       1.9900
                                                                1.3354 0.3861 1.0045
 0.1900 1.3354 0.3847 1.0009
                                                        2.0000 1.3354 0.3861 1.0045
 0.2000 1.3354 0.3847 1.0009
```

Figure 7. The variation of the mass M(t), energy E(t) and the relative energy E(t)/E(0) over time at  $\alpha = 1, q = 6$  but  $\gamma = 1, \beta = 0.1$ .

• Case IV: For  $\alpha = 1$  and q = 8, we have noticed a slight change in the  $H^2$  norm, particularly its relative quantity to the  $H^2$ -norm of the initial data. Consequently, as will be seen in the Case IV, by increasing the value of  $\alpha$ . This change can be controlled as  $\alpha/q$  slightly gets closer to 1. This confirms stable evolution of u(t,x) in time t.

```
Controlling nonlinear Growth for alpha =1.00, q =8.00, alpha/q = 0.1250 1.8000 1.3360 0.3758 1.0005
                                                         1.8100 1.3360 0.3758 1.0005
     Mass Energy Rel.
0.0100 1.3360 0.3756 1.0000
                                                         1.8200 1.3360 0.3758 1.0005
0.0200 1.3360 0.3756 1.0000
                                                         1.8300 1.3360 0.3758 1.0005
0.0300 1.3360 0.3756 1.0000
                                                         1.8400 1.3360 0.3758 1.0005
0.0400 1.3360 0.3756 1.0000
                                                         1.8500 1.3360 0.3758 1.0005
0.0500 1.3360 0.3756 1.0000
                                                         1.8600 1.3360 0.3758 1.0005
0.0600 1.3360 0.3756 1.0000
                                                         1.8700
                                                                  1.3360 0.3758 1.0005
0.0700 1.3360 0.3756 1.0000
                                                         1.8800 1.3360 0.3758 1.0005
0.0800 1.3360 0.3756 1.0000
                                                         1.8900 1.3360 0.3758 1.0005
0.0900 1.3360 0.3756 1.0000
                                                         1.9000 1.3360 0.3758 1.0005
0.1000 1.3360 0.3756 1.0000
                                                         1.9100 1.3360 0.3758 1.0005
0.1100 1.3360 0.3756 0.9999
                                                         1.9200 1.3360 0.3758 1.0005
0.1200 1.3360 0.3756 0.9999
                                                         1.9300 1.3360 0.3758 1.0005
0.1300 1.3360 0.3756 0.9999
                                                         1.9400 1.3360 0.3758 1.0005
0.1400 1.3360 0.3756 0.9999
                                                         1.9500
                                                                  1.3360 0.3758 1.0005
0.1500 1.3360 0.3756 0.9999
                                                                  1.3360 0.3758 1.0005
                                                         1.9600
0.1600 1.3360 0.3756 0.9999
                                                         1.9700 1.3360 0.3758 1.0005
0.1700 1.3360 0.3756 0.9999
                                                         1.9800 1.3360 0.3758 1.0004
0.1800 1.3360 0.3756 0.9999
                                                         1.9900 1.3360 0.3758 1.0004
0.1900 1.3360 0.3756 0.9999
                                                         2.0000 1.3360 0.3758 1.0004
0.2000 1.3360 0.3756 0.9999
```

Figure 8. Table showing the variation of the mass M(t), energy E(t) and the relative energy E(t)/E(0) over time at  $\alpha = 1, q = 8$  but  $\gamma = 1, \beta = 0.1$ .

• Case V: For  $\alpha = 4$  and q = 8, we have  $\alpha/q = 0.5$  but somewhat stable  $H^2$ -norm:

```
Controlling nonlinear Growth for alpha =4.00, q = 8.00, alpha/q = 0.5000 1.8000 1.3635 0.4530 0.9953
                                                         1.8100 1.3635 0.4528 0.9950
            Energy Rel.
                                                         1.8200 1.3635 0.4527 0.9947
0.0100 1.3635 0.4551 1.0000
0.0200 1.3635 0.4551 1.0000
                                                         1.8300 1.3635 0.4526 0.9945
0.0300 1.3635 0.4551 1.0000
                                                         1.8400 1.3635 0.4525 0.9942
0.0400 1.3635 0.4551 0.9999
                                                        1.8500 1.3635 0.4523 0.9939
0.0500 1.3635 0.4551 0.9999
                                                        1.8600 1.3635 0.4522 0.9936
0.0600 1.3635 0.4551 0.9999
                                                        1.8700 1.3635 0.4521 0.9933
0.0700 1.3635 0.4551 0.9999
                                                        1.8800 1.3635 0.4519 0.9930
0.0800 1.3635 0.4551 0.9999
                                                         1.8900
                                                                  1.3635 0.4518 0.9926
0.0900 1.3635 0.4551 0.9999
                                                         1.9000
                                                                  1.3635 0.4516 0.9923
0.1000 1.3635 0.4551 0.9999
                                                         1.9100 1.3635 0.4515 0.9920
0.1100 1.3635 0.4551 0.9999
0.1200 1.3635 0.4551 0.9999
                                                        1.9200 1.3635 0.4513 0.9916
0.1300 1.3635 0.4550 0.9999
                                                        1.9300 1.3635 0.4511 0.9913
0.1400 1.3635 0.4550 0.9999
                                                        1.9400 1.3635 0.4510 0.9909
0.1500 1.3635 0.4550 0.9999
                                                        1.9500 1.3635 0.4508 0.9906
0.1600 1.3635 0.4550 0.9999
                                                         1.9600 1.3635 0.4507 0.9902
0.1700 1.3635 0.4551 0.9999
                                                         1.9700 1.3635 0.4505 0.9898
0.1800 1.3635 0.4551 0.9999
                                                         1.9800 1.3635 0.4503 0.9895
0.1900 1.3635 0.4551 0.9999
                                                         1.9900
                                                                  1.3635 0.4501 0.9891
0.2000 1.3635 0.4551 0.9999
                                                         2.0000 1.3635 0.4500 0.9887
0.2100 1.3635 0.4551 0.9999
```

Figure 9. Table showing the variation of the mass M(t), energy E(t) and the relative energy E(t)/E(0) over time at  $\alpha = 4$ , q = 2 but  $\gamma = 8$ ,  $\beta = 0.1$ .

This indicate that as when  $\alpha/q \to 1$ , then u(t) tends to stable solutions as t increases. That is to say dispersion takes over. And nonlinearity takes control whenever  $\alpha/q \to 0$  as shown in the Figure of case II, Fig. 6.

5.2. **Dispersive effects.** For the dispersive effect, the time t, mass M(t), energy E(t) and the relative energy E(t)/E(0) are computed. We track the value of the energy and its relative variations over time t. The result is shown while the dispersive parameters  $\beta$  and  $\gamma$  vary.

For fixed nonlinear parameters  $\alpha = 1$  and q = 2, we perform the variation of the dispersive parameters  $\beta$  and  $\gamma$  as follows for  $\beta \in (0.1, 1)$  and  $\gamma \in (0.1, 1)$ .

• Case I: With the fixed values of  $\alpha$  and q, we vary the values of  $\beta$  and track the ratio  $\beta/\gamma$ . Here, we take  $\beta = 0.1$  and  $\gamma = 0.1$ , mass evolution undergoes slight deviation away from the initial mass but the energy indicates significant variation from the initial energy. The  $H^2$ -norm exhibits significant deviation as well, however, finite.

```
Controlling Dispersive effectsfor beta =0.10, gamma =0.10, beta/gamma = 1.0000 1.80000 1.85019 0.68886 1.53170 169947886.38998 1.01853
0.01000 1.33341 0.44981 1.00015 173100570.10940 0.99998
                                                                              1.82000 1.35046 0.69419 1.54354 169901131.18651 1.01881
0.02000 1.33348 0.44988 1.00032 173104519.00295 0.99995
                                                                             1.83000 1.35059 0.69687 1.54949 169878015.40018 1.01894
0.03000 1.33356 0.44998 1.00053 173108140.77376 0.99993
                                                                              1.84000 1.35073 0.69955 1.55546 169855078.11556 1.01908
0.04000 1.33363 0.45009 1.00077 173111443.63611 0.99991
                                                                              1.85000 1.35087 0.70224 1.56144 169832342.70543 1.01922
0.05000 1.33370 0.45021 1.00104 173114426.08056 0.99990
                                                                              1.86000 1.35100 0.70494 1.56743 169809802.09706 1.01935
0.06000 1.33378 0.45034 1.00134 173117086.77186 0.99988
                                                                               1.87000 1.35114 0.70764 1.57343 169787458.95745 1.01949
0.07000 1.33385 0.45049 1.00167 173119436.66843 0.99987
                                                                               1.88000 1.35128 0.71034 1.57945 169765328.24146 1.01962
0.08000 1.33393 0.45066 1.00204 173121453.46486 0.99985
                                                                              1.89000 1.35142 0.71305 1.58547 169743405.00996 1.01975
0.09000 1.33400 0.45083 1.00243 173123159.94713 0.99984
                                                                              1.90000 1.35156 0.71576 1.59149 169721688.53334 1.01988
0.10000 1.33407 0.45103 1.00286 173124519.67149 0.99984
                                                                              1.91000 1.35171 0.71847 1.59752 169700188.83974 1.02001
0.11000 1.33415 0.45123 1.00331 173125556.15275 0.99983
                                                                              1.92000 1.35185 0.72118 1.60356 169678898.95778 1.02014
0.12000 1.33422 0.45145 1.00380 173126259.64171 0.99983
                                                                              1.93000 1.35199 0.72390 1.60959 169657828.29509 1.02027
0.13000 1.33430 0.45168 1.00432 173126605.75174 0.99982
                                                                              1.94000 1.35214 0.72661 1.61562 169636971.27854 1.02039
0.14000 1.33437 0.45193 1.00487 173126599.64519 0.99982
                                                                              1,95000 1,35228 0,72932 1,62166 169616330,48428 1,02052
0.15000 1.33445 0.45219 1.00544 173126251.36589 0.99983
                                                                              1.96000 1.35243 0.73204 1.62769 169595902.83432 1.02064
0.16000 1.33452 0.45246 1.00605 173125551.50542 0.99983
                                                                               1.97000 1.35257 0.73475 1.63372 169575689.81354 1.02076
0.17000 1.33459 0.45275 1.00669 173124487.38999 0.99984
                                                                              1.98000 1.35272 0.73746 1.63975 169555684.74199 1.02088
0.18000 1.33467 0.45305 1.00736 173123057.85399 0.99985
                                                                              1.99000 1.35287 0.74017 1.64577 169535897.39017 1.02100
0.19000 1.33474 0.45336 1.00805 173121258.58394 0.99986
                                                                               2.00000 1.35302 0.74287 1.65179 169516322.92916 1.02112
0.20000 1.33482 0.45369 1.00878 173119092.69365 0.99987
```

Figure 10. Mass M(t), energy E(t) and the relative energy E(t)/E(0) over time for  $\beta = 0.1, \gamma = 0.1$ .

• Case II: For  $\beta=0.1$  and  $\gamma=0.5$ , the  $H^2$ -norm behaves well for a short time t but shows significant change as t increases. Similar behaviour is observed as in the case I. However, the mass and the evolutions exhibit slight deviation . Therefore, increase the value of  $\gamma$  lead to significant change in the associated conserved quantities.

Figure 11. Evolution of the mass M(t), energy E(t) and the relative energy E(t)/E(0) over time at  $\beta = 0.1, \gamma = 0.5$ .

• Case III: For  $\alpha = 1$  and q = 2,  $\beta = 0.3$  and  $\gamma = 0.1$ , we have the following results:

Figure 12. The variation of the mass M(t), energy E(t) and the relative energy E(t)/E(0) over time at  $\beta = 0.3$ ,  $\gamma = 0.1$ .

• **Case IV:** For  $\beta = 0.5$  and  $\gamma = 0.7$ , there is significant increase in the conserved quantities as well as the associated norms.

Figure 13. Variation of the mass M(t), energy E(t) and the relative energy E(t)/E(0) over time at  $\beta = 0.5$ ,  $\gamma = 0.7$ .

• Case V For  $\alpha = 1$  and q = 2,  $\beta = 0.9$  and  $\gamma = 0.9$ , we have the following results:

Figure 14. Variation of the mass M(t), energy E(t) and the relative energy  $H^2(t)/H^2(0)$  over time at  $\alpha = 0.9$ ,  $\gamma = 0.9$ .

Depending on how  $\beta/\gamma$  tends to 1, the evolutions tends to an unstable behaviour.

5.3. **Effect of radiative initial data.** These are initial conditions for which the underlying dynamical equation posses the tendency to generate radiation. That is the solution carries the energy to infinity dispersively. Theoretical background hinted having non-compactly supported radiative

initial data decays slowly or algebraically. Such initial data include those with oscillatory decay:  $\sin(2x)/(1+x^2)$  or those partially localized but posses radiative tail:  $\operatorname{sech}^2(x) + \varepsilon \cos(\pi x)e^{-x^2}$ .

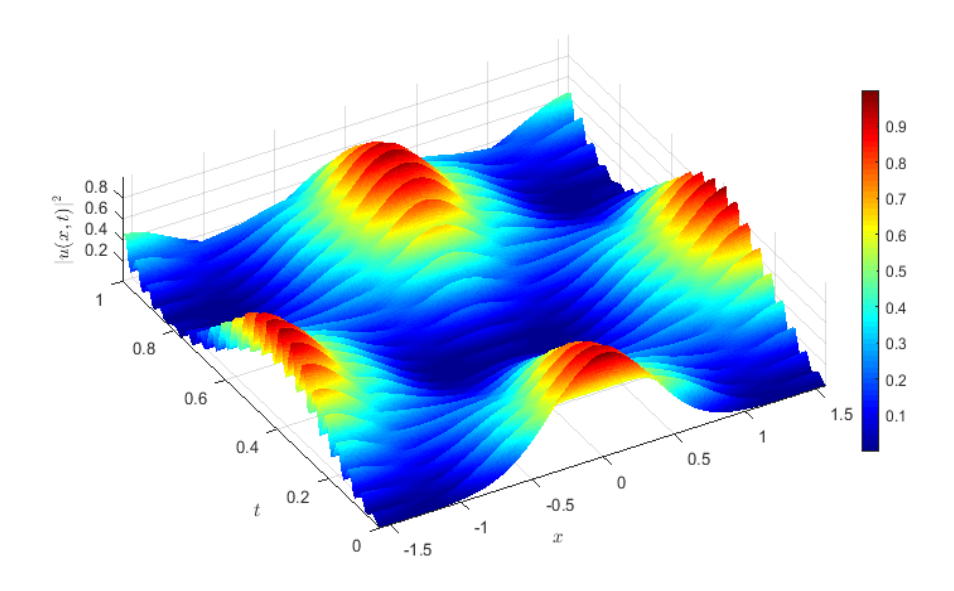


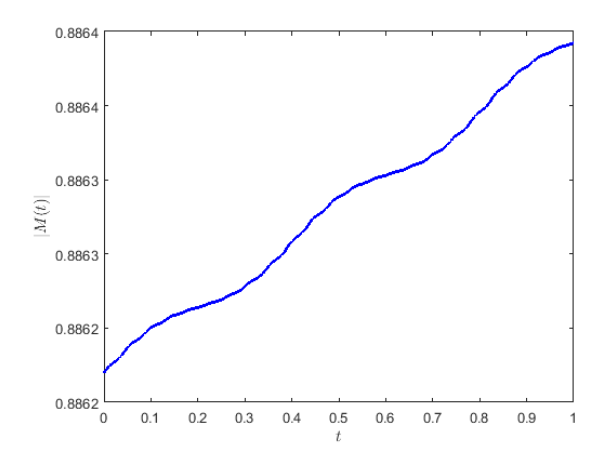
Figure 15. The evolution of the radiative initial data  $u_0(x) = \operatorname{sech}^2(x) + \varepsilon \cos(\pi x)e^{-x^2}$ .

In the table below, the dispersive effects of radiative initial data for  $\beta = 0.60$ ,  $\gamma = 0.40$ ,  $\beta/\gamma = 1.5$  is shown for the radiative initial data  $\mathrm{sech}^2(x) + \varepsilon \cos(\pi x)e^{-x^2}$ . The See Fig.15.

The radiative initial data appears to evolved by the underlying Schrödinger equation into some sort of breathers. To track the stability, we trace the evolution of the mass, energy as well as the  $H^2$ -norm and shows quasi-stable nature. Relative energy  $E_r(t)$  is also computed thereby confirming the relative errors encountered numerically.

Time: t	Mass: $M(t)$	Energy: $E(t)$	Rel. Energy: $E_r(t)$	$H^2(u(t))$	$H^2(u_0)/H^2(u(t))$
0.00100	0.88622	6.24201e+00	2.50470	3.70444e+00	1.00018
0.00200	0.88622	6.23350e+00	0.13990	3.70331e+00	1.00048
0.00300	0.88622	6.22307e+00	0.17124	3.70202e+00	1.00083
0.00400	0.88622	6.21251e+00	0.17329	3.70073e+00	1.00118
0.00500	0.88622	6.20241e+00	0.16600	3.69948e+00	1.00152
0.00600	0.88622	6.19263e+00	0.16061	3.69825e+00	1.00185
0.00700	0.88622	6.18198e+00	0.17481	3.69686e+00	1.00223
0.00800	0.88622	6.16940e+00	0.20653	3.69522e+00	1.00268
0.00900	0.88622	6.15483e+00	0.23937	3.69334e+00	1.00318
0.01000	0.88622	6.13910e+00	0.25821	3.69138e+00	1.00372
:	:	:	:	:	:
0.99000	0.88644	5.90902e+00	0.07954	3.65327e+00	1.01419
0.99100	0.88644	5.91254e+00	0.05777	3.65368e+00	1.01407
0.99200	0.88644	5.91550e+00	0.04862	3.65405e+00	1.01397
0.99300	0.88644	5.91888e+00	0.05560	3.65451e+00	1.01385
0.99400	0.88644	5.92341e+00	0.07429	3.65510e+00	1.01368
0.99500	0.88644	5.92902e+00	0.09211	3.65581e+00	1.01348
0.99600	0.88644	5.93436e+00	0.08772	3.65642e+00	1.01331
0.99700	0.88644	5.93790e+00	0.05815	3.65678e+00	1.01322
0.99800	0.88644	5.93887e+00	0.01600	3.65681e+00	1.01321
0.99900	0.88644	5.93739e+00	0.02442	3.65655e+00	1.01328
1.00000	0.88644	5.93463e+00	0.04525	3.65617e+00	1.01338

Likewise, the evolution of the mass and energy of the radiative initial data are described in the Fig. 16. The evolution of both quantities reflects the radiative property.



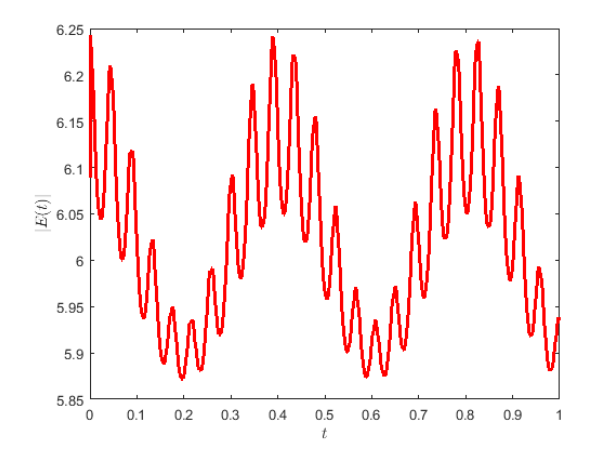


Figure 16. The evolution of mass and energy of the radiative initial data  $u_0(x) = \mathrm{sech}^2(x) + \varepsilon \cos(\pi x)e^{-x^2}$  with  $\beta = 0.6$ ,  $\gamma = 0.4$ .

5.4. **Discussion.** The ratio  $\beta/\gamma$  controls the dominance of high-order dispersion. Larger  $\beta$  values lead to stronger smoothing effects, stabilizing the solution. The ratio  $\alpha/q$  determines the nonlinear

intensity. For moderate values, the energy functional remains conserved, ensuring bounded growth. These results are shown in tabular form as described.

It's been seen, in section 5.1, that stability of the solution is guaranteed as the ratio  $\alpha/q \to 1$  (i.e. tends to 1). This is evident from the tables in the cases I, II, III, and IV, where the nonlinearity related paramters  $\alpha$  and q are varied. In these cases, the mass, energy and the  $H^2$ -norms stays finite with little significant deviation with increase in the time parameter. However, the case V where  $\alpha=4$  and q=8 signals the tendency of singular solutions the conserved quantities as well as the norms tend to increase significantly. As a result, stability of the solution cannot be affirmed when  $\alpha/q\to 0$ . This is due to the fact that the dispersion coefficients  $\beta$  and  $\gamma$  are kept small.

On the other hand, keeping the nonlinearity related parameters  $\alpha=1$  and q=2 fixed, varying dispersive parameters  $\beta$  and  $\gamma$  could yield to uncontrolled quantities. As indicated in the section 5.2, the dispersive parameters effects depends on how  $\beta/\gamma$  approaches 1. Significant variation is noticed when the quantity  $\beta/\gamma \to 1$  when both  $\beta$  and  $\gamma$  are bigger as can be seen in Case I and V where the  $H^2$ -norm relative ratio is much greater than 1. Hence, instability is bound to kick in particularly in the case similar to the former (14) in comparison to the latter table (10). The only case one gets stable behaviour in the mass, energy and the  $H^2$ -norms is case II of (5.2). Unstable behaviour is present in the other cases.

For radiative type of initial data, we observed the remarkable behaviour as shown in Fig. 15 where  $\beta > \gamma$  with q=2 and these is maintained throughout the evolution as  $t\to\infty$ . As it is expected, when radiation is present, the associated conserved quantities such as mass and energy may exhibit otherwise kind of behaviour. This can be seen in the Figures of Fig. 16 where the mass and the energy posses non-constant evolutions.

#### 6. Summary and Conclusion

This study presents the study effects of involved dispersive and nonlinearity parameters for a a localized and radiative initial data for a general one dimensional fourth order nonlinear Schrödinger equation numerically. An IMEX splitting method is used to solve the FNSE for efficiency. IMEX split method involves splitting the equation into linear and nonlinear components. We study establishes the balance between stability and efficiency of the solutions based on the tracking the evolution of mass, energy and  $H^2$ -norms. Stable and unstable behaviour are observed in both effects of dispersion and nonlinearity for a localized type of initial data. On the other hand, radiative initial data (localized wave with radiative tail) leads to the remarkable wave behaviour known as breathers.

Future work will explore adaptive time-stepping and higher-order schemes for more complex systems like two dimensional version. Such schemes if implemented would present clear and reliable result especially in the higher dimensional problem. Such equations are important in application, especially considering the origin of the main equation in the field of quantum mechanics which later finds application in nonlinear optics.

#### 7. Appendix I: Preliminaries

We define the norms used:

• The Sobolev  $H^2$ -norm:

$$||u||_{H^2}^2 = ||u||_{L^2}^2 + ||\partial_x u||_{L^2}^2 + ||\partial_x^2 u||_{L^2}^2.$$

• The  $L^{\infty}$ -norm:

$$||u||_{L^{\infty}} = \sup_{x \in \mathbb{R}} |u(x)|.$$

By Sobolev embedding, we know:

$$||u||_{L^\infty} \leq C||u||_{H^2},$$

where C > 0 is a constant dependent on the embedding.

Appendix II: Lagrangian Formulation of the Equation

The fourth-order Schrödinger equation is given as:

$$iu_t + \beta \partial_x^4 u + \gamma \partial_x^2 u + \alpha |u|^q u = 0.$$

Lagrangian Density. The associated Lagrangian density and its Hamiltonian density are:

$$\mathcal{L} = \frac{i}{2} \left( u^* u_t - u u_t^* \right) + \beta |\partial_x^2 u|^2 - \gamma |\partial_x u|^2 + \frac{2\alpha}{q+2} |u|^{q+2};$$

$$\mathcal{H} = \Pi \cdot \dot{u} - \mathcal{L} = u_t \frac{\partial \mathcal{L}}{\partial u_t^*} - \mathcal{L} = \gamma |u_x|^2 - \beta |u_{xx}|^2 - \frac{2\alpha}{(q+2)} |u|^{q+2}.$$

where  $u^*$  is the complex conjugate of u,  $|\partial_x^2 u|^2 = (\partial_x^2 u)(\partial_x^2 u^*)$ ,  $|\partial_x u|^2 = (\partial_x u)(\partial_x u^*)$ , and the nonlinear term contributes  $-\frac{\alpha}{q+2}|u|^{q+2}$ . Here for the equation:

- The first term represents the dynamical evolution of the field.
- The second and third terms correspond to the fourth- and second-order spatial derivatives, respectively.
- The fourth term represents the nonlinear interaction.

## Appendix III

Consider the fourth-order Schrödinger equation:

$$iu_t + \mathcal{L}_4 u + \alpha |u|^q u = 0, \quad \mathcal{L}_4 = \beta \partial_x^4 + \gamma \partial_x^2.$$

The energy functional for the main equation is as given in (2.2) Then one may rigorously prove the boundedness of  $||u||_{L^{\infty}}$  and  $||u||_{H^2}$  in terms of the energy functional E(u).

#### Conservation of Mass and Energy

The mass function M(t) over time is defined by

$$M(t) = \int_{\mathbb{R}} |u(t,x)|^2 = ||u||$$

and the energy functional E(u) defined (2.2). If these two quantities are conserved over time t, then we are bound to have:

$$\frac{dM(u(t))}{dt} = 0, \qquad \frac{dE(u)}{dt} = 0.$$

The proof follows from multiplying the equation by  $u^*$ , integrating by parts, and using boundary conditions.

## 7.1. Proof of Boundedness.

*Proof.* 1. Control of  $H^2$ -norm: From the energy functional (2.2), one uses the Sobolev inequality  $||u||_{L^{\infty}} \le C||u||_{H^2}$ , it follows that:

$$||u||_{H^2}^2 \le CE(u).$$

2. Control of  $L^{\infty}$ -norm: Again, using Sobolev embedding, we directly have:

$$||u||_{L^\infty} \leq C'||u||_{H^2}.$$

Since  $||u||_{H^2}^2 \le CE(u)$ , it follows that:

$$||u||_{L^{\infty}} \leq C' E(u)^{1/2}.$$

Thus, the solution is bounded in  $H^2$  and  $L^{\infty}$ .

## APPENDIX IV: CONTROL ANALYSIS ALGORITHM

## Algorithm 1: Stability Tracking of Dispersive Effects ( $\beta/\gamma$ ).

**Mathematical Formulation.** The stability of the dispersive effects is analyzed by monitoring the  $H^2$ -norm of the solution, which is bounded by the Sobolev embedding theorem:

$$||u||_{L^{\infty}} \le C||u||_{H^2}. \tag{7.1}$$

We decompose the equation into linear and nonlinear parts:

$$iu_t + \mathcal{L}_4 u = 0, \quad iu_t + \alpha |u|^q u = 0.$$
 (7.2)

The linear evolution is solved using a spectral method, which efficiently handles the dispersive operators.

## Algorithm Steps.

- (1) 1. Define the initial condition  $u_0$  and parameters  $\beta$ ,  $\gamma$ , and domain size L.
- (2) Compute the Fourier transform of u and the linear operators  $k^2$  and  $k^4$ .
- (3) Solve the linear evolution using a fourth-order Runge-Kutta (RK4) method.
- (4) Track the  $H^2$ -norm of the solution over time:

$$H^{2}(u) = ||u||^{2} + ||\partial_{x}u||^{2} + ||\partial_{x}^{2}u||^{2}.$$
(7.3)

## **Algorithm 2: Nonlinear Growth Control (** $\alpha$ /q**).**

*Mathematical Formulation.* The nonlinear term  $\alpha |u|^q u$  introduces growth that is controlled using the energy functional (2.2). Then the energy conservation is monitored to ensure that:

$$\frac{dE[u]}{dt} = 0. (7.4)$$

Sobolev embedding ensures control over the  $L^{\infty}$ -norm of u:

$$||u||_{L^{\infty}}^{q} \le C||u||_{H^{2}}^{q}. \tag{7.5}$$

## Algorithm Steps.

- (1) Define the initial condition  $u_0$  and parameters  $\alpha$ , q,  $\beta$ , and  $\gamma$ .
- (2) Decompose the evolution into linear and nonlinear parts.
- (3) Solve the nonlinear evolution using the Duhamel principle:

$$u(t) = e^{-i\mathcal{L}_4 t} u_0 - i \int_0^t e^{-i\mathcal{L}_4 (t-s)} \alpha |u|^q u \, ds.$$
 (7.6)

(4) Track energy conservation and ensure that it remains constant.

#### MATLAB Codes

```
L = 4*pi; % Domain length
N = 2^10; % Number of spatial points
tmax = 4*0.5; % Final time
dt = 0.01; % Time step size
% Spatial grid and wavenumbers
x = linspace(-L/2, L/2, N)'; % spatial variables
dx = x(2) - x(1); % step size
kx = (2 * pi / (2 * L)) * [0:(N/2-1) -N/2:-1]'; % Fourier wavenumbers
% Initial condition (e.g., Schwartzian data)
%u0 = exp(-x.^2); % Schwartzian function
u0 = sech(x-1).^2; % Schwartzian function (initial data)
%A = 0.25; B = 0.25; u0 = 4*(A*sech(0.5*A^2*(x-4)).^2+B*sech(0.5*B^2*(x+4))
   ).^2); % Schwartzian function
% Precompute linear operator in Fourier space
L4x = (beta * kx.^4 - gamma * kx.^2); % spatial linear operator in Fourier
    space
L4 = 1i * L4x; % Complete Linear part
% Time-stepping loop using IMEX splitting
u = u0; % Initialize solution
u_hat = fft(u); % Fourier transform of initial condition
t = 0:dt:tmax; % Time vector
% Initialize mass and energy trackers
mass = zeros(1, length(t));
energy = zeros(1, length(t));
% Store solution for visualization
solution = zeros(N, length(t));
solution(:, 1) = u;
% Define the range of alppha and q
alpha_values = [0.5, 1, 2, 4];
```

```
q_{values} = [2,4,6,8];
labels ={'Time' 'Mass' 'Energy' 'Rel._Energy'};
% Loop over alpha/q values
for alpha = alpha_values
for q = q_values
% initialize the solutoion and compute initial mass and initial
% energy
% Compute initial mass and energy
mass(1) = sum(abs(u).^2) * dx; % Mass: ||u||_2^2
energy(1) = sum(-beta * abs(ifft(1i*kx.*fft(1i*kx.*fft(u))))).^2 ...
+ gamma * abs(ifft(1i*kx.*fft(u))).^2 ...
-2 * (alpha/(q+2)) * abs(u).^(q+2)) * dx; % Energy
fprintf('Controlling_nonlinear_Growth_for_alpha_=%.2f,_q_=%.2f,_alpha/q_=_
   %.4f\n', alpha,q, alpha/q);
fprintf('%-6s___,%-6s__,%-5.5s\n', labels{:});
for n = 2:length(t)
% Implicit linear step (solve exactly in Fourier space)
u_hat = exp(dt * L4) .* u_hat;
% Transform back to physical space for nonlinear step
u = ifft(u_hat);
% Explicit nonlinear step
u = u - 1i * dt * alpha * u .* abs(u).^q;
% Transform back to Fourier space for the next step
u_hat = fft(u);
% Compute mass and energy at this time step
mass(n) = sum(abs(u).^2) * dx; % Mass: ||u||_2^2
energy(n) = sum(-beta * abs(ifft(1i*kx.*fft(ifft(1i*kx.*fft(u))))).^2 ...
+ gamma * abs(ifft(1i*kx.*fft(u))).^2 ...
- (2 * alpha/(q+2)) * abs(u).^(q+2)) * dx; % Energy
% Store solution
solution(:, n) = (u);
```

```
% fprintf('Time: %.2f, Mass: %.2f, Energy: %.2f, Rel. Energy: %.2f\n', t(n
                       ), mass(n), abs(energy(n)), abs(energy(n)/energy(1)));
fprintf('%-\Box.4f\Box-.4f\Box-.4f\Box-.4f\Box-.4f\Box-.4f\Box-.4f\Box-.4f\Box-.4f\Box-.4f\Box-.4f\Box-.4f\Box-.4f\Box-.4f\Box-.4f\Box-.4f\Box-.4f\Box-.4f\Box-.4f\Box-.4f\Box-.4f\Box-.4f\Box-.4f\Box-.4f\Box-.4f\Box-.4f\Box-.4f\Box-.4f\Box-.4f\Box-.4f\Box-.4f\Box-.4f\Box-.4f\Box-.4f\Box-.4f\Box-.4f\Box-.4f\Box-.4f\Box-.4f\Box-.4f\Box-.4f\Box-.4f\Box-.4f\Box-.4f\Box-.4f\Box-.4f\Box-.4f\Box-.4f\Box-.4f\Box-.4f\Box-.4f\Box-.4f\Box-.4f\Box-.4f\Box-.4f\Box-.4f\Box-.4f\Box-.4f\Box-.4f\Box-.4f\Box-.4f\Box-.4f\Box-.4f\Box-.4f\Box-.4f\Box-.4f\Box-.4f\Box-.4f\Box-.4f\Box-.4f\Box-.4f\Box-.4f\Box-.4f\Box-.4f\Box-.4f\Box-.4f\Box-.4f\Box-.4f\Box-.4f\Box-.4f\Box-.4f\Box-.4f\Box-.4f\Box-.4f\Box-.4f\Box-.4f\Box-.4f\Box-.4f\Box-.4f\Box-.4f\Box-.4f\Box-.4f\Box-.4f\Box-.4f\Box-.4f\Box-.4f\Box-.4f\Box-.4f\Box-.4f\Box-.4f\Box-.4f\Box-.4f\Box-.4f\Box-.4f\Box-.4f\Box-.4f\Box-.4f\Box-.4f\Box-.4f\Box-.4f\Box-.4f\Box-.4f\Box-.4f\Box-.4f\Box-.4f\Box-.4f\Box-.4f\Box-.4f\Box-.4f\Box-.4f\Box-.4f\Box-.4f\Box-.4f\Box-.4f\Box-.4f\Box-.4f\Box-.4f\Box-.4f\Box-.4f\Box-.4f\Box-.4f\Box-.4f\Box-.4f\Box-.4f\Box-.4f\Box-.4f\Box-.4f\Box-.4f\Box-.4f\Box-.4f\Box-.4f\Box-.4f\Box-.4f\Box-.4f\Box-.4f\Box-.4f\Box-.4f\Box-.4f\Box-.4f\Box-.4f\Box-.4f\Box-.4f\Box-.4f\Box-.4f\Box-.4f\Box-.4f\Box-.4f\Box-.4f\Box-.4f\Box-.4f\Box-.4f\Box-.4f\Box-.4f\Box-.4f\Box-.4f\Box-.4f\Box-.4f\Box-.4f\Box-.4f\Box-.4f\Box-.4f\Box-.4f\Box-.4f\Box-.4f\Box-.4f\Box-.4f\Box-.4f\Box-.4f\Box-.4f\Box-.4f\Box-.4f\Box-.4f\Box-.4f\Box-.4f\Box-.4f\Box-.4f\Box-.4f\Box-.4f\Box-.4f\Box-.4f\Box-.4f\Box-.4f\Box-.4f\Box-.4f\Box-.4f\Box-.4f\Box-.4f\Box-.4f\Box-.4f\Box-.4f\Box-.4f\Box-.4f\Box-.4f\Box-.4f\Box-.4f\Box-.4f\Box-.4f\Box-.4f\Box-.4f\Box-.4f\Box-.4f\Box-.4f\Box-.4f\Box-.4f\Box-.4f\Box-.4f\Box-.4f\Box-.4f\Box-.4f\Box-.4f\Box-.4f\Box-.4f\Box-.4f\Box-.4f\Box-.4f\Box-.4f\Box-.4f\Box-.4f\Box-.4f\Box-.4f\Box-.4f\Box-.4f\Box-.4f\Box-.4f\Box-.4f\Box-.4f\Box-.4f\Box-.4f\Box-.4f\Box-.4f\Box-.4f\Box-.4f\Box-.4f\Box-.4f\Box-.4f\Box-.4f\Box-.4f\Box-.4f\Box-.4f\Box-.4f\Box-.4f\Box-.4f\Box-.4f\Box-.4f\Box-.4f\Box-.4f\Box-.4f\Box-.4f\Box-.4f\Box-.4f\Box-.4f\Box-.4f\Box-.4f\Box-.4f\Box-.4f\Box-.4f\Box-.4f\Box-.4f\Box-.4f\Box-.4f\Box-.4f\Box-.4f\Box-.4f\Box-.4f\Box-.4f\Box-.4f\Box-.4f\Box-.4f\Box-.4f\Box-.4f\Box-.4f\Box-.4f\Box-.4f\Box-.4f\Box-.4f\Box-.4f\Box-.4f\Box-.4f\Box-.4f\Box-.4f\Box-.
                       abs(energy(n)/energy(1))]);
end
fprintf('\n');
end
% Visualization of the solution
  [X, T_grid] = meshgrid(x, t);
figure(1);
surf(X, T_grid, real(solution.'), 'EdgeColor', 'none');
colormap jet;
xlabel('$x$', Intp, Ltx);
ylabel('$t$', Intp, Ltx);
zlabel('$u(x,\(\_\)$', Intp, Ltx);
\label{local}  \textbf{title}('$iu_t+\mathbf{L}_4u+\mathbf{N}[u]=0,\_\\quad\_\\alpha\_=\_2,\_\\beta\_=0.1,\_\\quad\_=0.1,\_\\quad\_=0.1,\_\\quad\_=0.1,\_\\quad\_=0.1,\_\\quad\_=0.1,\_\\quad\_=0.1,\_\\quad\_=0.1,\_\\quad\_=0.1,\_\\quad\_=0.1,\_\\quad\_=0.1,\_\\quad\_=0.1,\_\\quad\_=0.1,\_\\quad\_=0.1,\_\\quad\_=0.1,\_\\quad\_=0.1,\_\\quad\_=0.1,\_\\quad\_=0.1,\_\\quad\_=0.1,\_\\quad\_=0.1,\_\\quad\_=0.1,\_\\quad\_=0.1,\_\\quad\_=0.1,\_\\quad\_=0.1,\_\\quad\_=0.1,\_\\quad\_=0.1,\_\\quad\_=0.1,\_\\quad\_=0.1,\_\\quad\_=0.1,\_\\quad\_=0.1,\_\\quad\_=0.1,\_\\quad\_=0.1,\_\\quad\_=0.1,\_\\quad\_=0.1,\_\\quad\_=0.1,\_\\quad\_=0.1,\_\\quad\_=0.1,\_\\quad\_=0.1,\_\\quad\_=0.1,\_\\quad\_=0.1,\_\\quad\_=0.1,\_\\quad\_=0.1,\_\\quad\_=0.1,\_\\quad\_=0.1,\_\\quad\_=0.1,\_\\quad\_=0.1,\_\\quad\_=0.1,\_\\quad\_=0.1,\_\\quad\_=0.1,\_\\quad\_=0.1,\_\\quad=0.1,\_\\quad=0.1,\_\\quad=0.1,\_\\quad=0.1,\_\\quad=0.1,\_\\quad=0.1,\_\\quad=0.1,\_\\quad=0.1,\_\\quad=0.1,\_\\quad=0.1,\_\\quad=0.1,\_\\quad=0.1,\_\\quad=0.1,\_\\quad=0.1,\_\\quad=0.1,\_\\quad=0.1,\_\\quad=0.1,\_\\quad=0.1,\_\\quad=0.1,\_\\quad=0.1,\_\\quad=0.1,\_\\quad=0.1,\_\\quad=0.1,\_\\quad=0.1,\_\\quad=0.1,\_\\quad=0.1,\_\\quad=0.1,\_\\quad=0.1,\_\\quad=0.1,\_\\quad=0.1,\_\\quad=0.1,\_\\quad=0.1,\_\\quad=0.1,\_\\quad=0.1,\_\\quad=0.1,\_\\quad=0.1,\_\\quad=0.1,\_\\quad=0.1,\_\\quad=0.1,\_\\quad=0.1,\_\\quad=0.1,\_\\quad=0.1,\_\\quad=0.1,\_\\quad=0.1,\_\\quad=0.1,\_\\quad=0.1,\_\\quad=0.1,\_\\quad=0.1,\_\\quad=0.1,\_\\quad=0.1,\_\\quad=0.1,\_\\quad=0.1,\_\\quad=0.1,\_\\quad=0.1,\_\\quad=0.1,\_\\quad=0.1,\_\\quad=0.1,\_\\quad=0.1,\_\\quad=0.1,\_\\quad=0.1,\_\\quad=0.1,\_\\quad=0.1,\_\\quad=0.1,\_\\quad=0.1,\_\\quad=0.1,\_\\quad=0.1,\_\\quad=0.1,\_\\quad=0.1,\_\\quad=0.1,\_\\quad=0.1,\_\\quad=0.1,\_\\quad=0.1,\_\\quad=0.1,\_\\quad=0.1,\_\\quad=0.1,\_\\quad=0.1,\_\\quad=0.1,\_\\quad=0.1,\_\\quad=0.1,\_\\quad=0.1,\_\\quad=0.1,\_\\quad=0.1,\_\\quad=0.1,\_\\quad=0.1,\_\\quad=0.1,\_\\quad=0.1,\_\\quad=0.1,\_\\quad=0.1,\_\\quad=0.1,\_\\quad=0.1,\_\\quad=0.1,\_\\quad=0.1,\_\\quad=0.1,\_\\quad=0.1,\_\\quad=0.1,\_\\quad=0.1,\_\\quad=0.1,\_\\quad=0.1,\_\\quad=0.1,\_\\quad=0.1,\_\\quad=0.1,\_\\quad=0.1,\_\\quad=0.1,\_\\quad=0.1,\_\\quad=0.1,\_\\quad=0.1,\_\\quad=0.1,\_\\quad=0.1,\_\\quad=0.1,\_\\quad=0.1,\_\\quad=0.1,\_\\quad=0.1,\_\\quad=0.1,\_\\quad=0.1,\_\\quad=0.1,\_\\quad=0.1,\_\\quad=0.1,\_\\quad=0.1,\_\\quad=0.1,\_\\quad=0.1,\_\\quad=0.1,\_\\quad=0.1,\_\\quad=0.1,\_\\quad=0.1,\_\\quad=0.1,\_\\
                       _1$', Intp, Ltx);
view([-30, 70]);
colorbar;
axis tight;
% Plot mass and energy over time
figure(2);
plot(t, abs(mass), 'b', 'LineWidth', 2);
%hold on;
%legend('Mass', 'Energy');
xlabel('$t$', Intp, Ltx);
ylabel('$M(t)$', Intp, Ltx);
title('Mass_Conservation');
grid on;
figure(3)
plot(t, abs(energy), 'r', 'LineWidth', 2);
xlabel('$t$', Intp, Ltx);
```

```
ylabel('$E(t)$', Intp, Ltx);
title('Energy_Conservation');
grid on;
end
```

```
% MATLAB Script for IMEX Splitting To Solve Fourth-Order nonlinear
   Schrdinger Equation
% i u_t+\beta = u^x = 0
% with Mass and Energy Conservation Tracking
%%%% Typesetting parameters
FS = 'FontSize'; Intp ='Interpreter'; Ltx = 'Latex';
format shortG
% Physical Parameters involved
%beta = 0.1; % Coefficient for u_xxxx term
%gamma = 1; % Coefficient for u_xx term
beta_values = 0.1:0.2:1;
gamma_values = 0.1:0.2:1;
alpha = 1; % Coefficient for nonlinear term
q = 2; % Power of the nonlinear term
L = 4*pi; % Domain length
N = 2^10; % Number of spatial points
tmax = 4*0.5; % Final time
dt = 0.01; % Time step size
% Spatial grid and wavenumbers
x = linspace(-L/2, L/2, N)'; % spatial variables
dx = x(2) - x(1); % step size
kx = (2 * pi / (2 * L)) * [0:(N/2-1) - N/2:-1]'; % Fourier wavenumbers
k2 = kx.^2; k4 = kx.^4;
% Initial condition (e.g., Schwartzian data)
%u0 = exp(-x.^2); % Schwartzian function
u0 = sech(x-1).^2; % Schwartzian function (initial data)
```

```
%A = 0.25; B = 0.25; u0 = 4*(A*sech(0.5*A^2*(x-4)).^2+B*sech(0.5*B^2*(x+4))
   ).^2); % Schwartzian function
% Time-stepping loop using IMEX splitting
u = u0; % Initialize solution
% H2_norm of the initial data
H2_0 = sqrt(sum((abs(u).^2 + abs(k2.*u).^2 + abs(k4.*u).^2) * dx));
u_hat = fft(u); % Fourier transform of initial condition
t = 0:dt:tmax; % Time vector
% Initialize mass and energy trackers
mass = zeros(1, length(t));
energy = zeros(1, length(t));
% Store solution for visualization
solution = zeros(N, length(t));
solution(:, 1) = u;
% Define the range of alppha and q
% alpha_values = [0.5, 1,2,4];
% q_{values} = [2,4,6,8];
labels ={'Time' 'Mass' 'Energy' 'Rel. _{\perp}Energy_{\perp}' '_{\perp}H^2(u(t))' 'H^2(t)/H^2(
   u_0)'};
% Loop over gamma/beta
for beta = beta_values
for gamma = gamma_values
% initialize the solutoion and compute initial mass and initial
% energy
% Compute initial mass and energy
mass(1) = sum(abs(u).^2) * dx; % Mass: ||u||_2^2
energy(1) = sum(-beta * abs(ifft(1i*kx.*fft(ifft(1i*kx.*fft(u))))).^2 ...
+ gamma * abs(ifft(1i*kx.*fft(u))).^2 ...
- 2 * (alpha/(q+2)) * abs(u).^(q+2)) * dx; % Energy
```

```
fprintf('Controlling_Dispersive_effectsfor_beta_=%.2f,_gamma_=%.2f,_beta/
   gamma_=_%.4f\n', beta,gamma, beta/gamma); %, H2_norm, H2_norm/H2_0
fprintf('%-6s___%-6s__%-6s__%-6s___%-6s__\n', labels{:});
% Precompute linear operator in Fourier space
L4 = 1i * (beta * kx.^4 - gamma * kx.^2);
for n = 2:length(t)
% Implicit linear step (solve exactly in Fourier space)
u_hat = exp(dt * L4) .* u_hat;
% Transform back to physical space for nonlinear step
u = ifft(u_hat);
% Explicit nonlinear step
u = u - 1i * dt * alpha * u .* abs(u).^q;
% Transform back to Fourier space for the next step
u_hat = fft(u);
% Compute mass and energy at this time step
mass(n) = sum(abs(u).^2) * dx; % Mass: ||u||_2^2
energy(n) = sum(-beta * abs(ifft(1i*kx.*fft(ifft(1i*kx.*fft(u))))).^2 ...
+ gamma * abs(ifft(1i*kx.*fft(u))).^2 ...
- (2 * alpha/(q+2)) * abs(u).^(q+2)) * dx; % Energy
% Store solution
solution(:, n) = (u);
sol_u = solution(:,n);
H2\_norm = sqrt(sum((abs(sol_u).^2 + abs(k2.*u).^2 + abs(k4.*u).^2) * dx));
% fprintf('Time: %.2f, Mass: %.2f, Energy: %.2f, Rel. Energy: %.2f\n', t(n
   ), mass(n), abs(energy(n)), abs(energy(n)/energy(1)));
fprintf('%-.5f__%-.5f__%-0.5f__%-0.5f__%-0.5f\n', ...
[t(n), mass(n), abs(energy(n)), abs(energy(n)/energy(1)),H2_norm, H2_0/
   H2_norm]);
% energy ratio should be relatively 1 (~ 1)
% H2 norm ratio should be finite
```

```
end
fprintf('\n');
end
% Visualization of the solution
[X, T_grid] = meshgrid(x, t);
figure(1);
surf(X, T_grid, real(solution.'), 'EdgeColor', 'none');
colormap jet;
xlabel('$x$', Intp, Ltx);
ylabel('$t$', Intp, Ltx);
zlabel('$u(x,\(\docume{t}\)$', Intp, Ltx);
title('siu_t+\mathcal{L}_4u+N[u]=0, \quad_\alpha==2, \beta=0.1, \quad=
   _1$', Intp, Ltx);
view([-30, 70]);
colorbar;
axis tight;
% Plot mass and energy over time
figure(2);
plot(t, abs(mass), 'b', 'LineWidth', 2);
%hold on;
%legend('Mass', 'Energy');
xlabel('$t$', Intp, Ltx);
ylabel('$M(t)$', Intp, Ltx);
title('Mass_Conservation');
grid on;
figure(3)
plot(t, abs(energy), 'r', 'LineWidth', 2);
xlabel('$t$', Intp, Ltx);
ylabel('$E(t)$', Intp, Ltx);
title('Energy_Conservation');
grid on;
end
```

#### Appendix V: Lie Symmetries of the equation

Investigating the lie symmetry groups of the FSE involves identifying continous symmetry of the equation.

Lie symmetry analysis focuses on finding transformation that leaves the PDE invariant. These transformations form a lie group, and the association infinitesimal generators form a lie algebra.

To find the lie symmetry of the FSE, we perform an infinitesimal transformation on the dependent variable U(x,t) and the independent variable x and t as follows:

$$u' = u + \epsilon \eta(x, t, u) \tag{7.7}$$

$$x' = x + \epsilon \zeta(x, t, u), \quad t' = t + \epsilon \tau(x, t, u) \tag{7.8}$$

where  $\epsilon$  is an infinitesimal parameter, and  $\zeta$ ,  $\tau$  and  $\eta$  are the infinitesimal generators.

The generators  $\zeta(x,t,u)$ ,  $\tau(x,t,u)$  and  $\eta(x,t,u)$  must satisfy the condition that the transformtion or the transformed FSE remained invariant. using the lie symmetry method, we can identify the following symmetries.

- 7.2. **Infinitesimal generators.** According to the symmetry of the equation, the following vector fields are generated
  - Time translation:  $X_1 = \frac{\partial}{\partial t}$ ;
  - Space translation:  $X_2 = \frac{\partial}{\partial x}$ ;
  - Phase symmetry:  $X_3 = iu \frac{\partial}{\partial u}$ ;
  - Galilean symmetry:  $X_4 = t \frac{\partial}{\partial x} + i(\frac{x}{2} + it)u \frac{\partial}{\partial u}$ ;
  - Scaling symmetry:

$$x' = \lambda^a x$$
,  $t' = \lambda^b t$ ,  $u'(x', t') = \lambda^c u(x, t)$ 

with the generator

$$X_5 = x \frac{\partial}{\partial x} + 2t \frac{\partial}{\partial t} - \frac{u}{2} \frac{\partial}{\partial u}$$
 (7.9)

**Definition 7.1** (Lie Algebra of the symmetries). *The associated symmetries form a lie algebra of generators:* 

$$(X_1, X_2, X_3, X_4, X_5)$$

The commutator of these generators provide the structure constants of the lie algebra.

$$[X_1, X_2] = 0$$
,  $[X_1, X_5] = -2X_1$ ,  $[X_2, X_4] = X_1$ 

Utilizing these Lie symmetries one may simplify the equation by reducing the number of independent variables it may have which in turn would lead to to the symmetry reduced solutions. It is known that equations that are *Galilean* invariant admits travelling wave solutions, *scale invariant* has self-similar solutions where the solutions shape is preserved while it grows or shrink over time. Likewise, for phase-invariance, the symmetry can lead to the identification of stationary solutions.

**Acknowledgments.** This work was supported and funded by the Deanship of Scientific Research at Imam Mohammad Ibn Saud Islamic University (IMSIU) (grant number IMSIU-DDRSP2501).

**Funding Statement.** This work was supported and funded by the Deanship of Scientific Research at Imam Mohammad Ibn Saud Islamic University (IMSIU) (grant number IMSIU-DDRSP2501).

**Conflicts of Interest:** The authors declare that there are no conflicts of interest regarding the publication of this paper.

#### References

- [1] F. Araruna, R. Capistrano-Filho, G. Doronin, Energy Decay for the Modified Kawahara Equation Posed in a Bounded Domain, J. Math. Anal. Appl. 385 (2012), 743–756. https://doi.org/10.1016/j.jmaa.2011.07.003.
- [2] U.M. Ascher, S.J. Ruuth, R.J. Spiteri, Implicit-explicit Runge-Kutta Methods for Time-Dependent Partial Differential Equations, Appl. Numer. Math. 25 (1997), 151–167. https://doi.org/10.1016/s0168-9274(97)00056-1.
- [3] U.M. Ascher, S.J. Ruuth, R.J. Spiteri, Implicit-explicit Runge-Kutta Methods for Time-Dependent Partial Differential Equations, Appl. Numer. Math. 25 (1997), 151–167. https://doi.org/10.1016/s0168-9274(97)00056-1.
- [4] J.C. Butcher, Numerical Methods for Ordinary Differential Equations, Wiley, 2016.
- [5] R.D.A. Capistrano–Filho, C. Kwak, F.J. Vielma Leal, On the Control Issues for Higher-Order Nonlinear Dispersive Equations on the Circle, Nonlinear Anal.: Real World Appl. 68 (2022), 103695. https://doi.org/10.1016/j.nonrwa. 2022.103695.
- [6] M.A. Caicedo, R. Capistrano Filho, B. Zhang, Neumann Boundary Controllability of the Korteweg–De Vries Equation on a Bounded Domain, SIAM J. Control. Optim. 55 (2017), 3503–3532. https://doi.org/10.1137/15m103755x.
- [7] R.A. Capistrano–Filho, A.F. Pazoto, L. Rosier, Control of a Boussinesq System of Kdv–Kdv Type on a Bounded Interval, ESAIM: Control. Optim. Calc. Var. 25 (2019), 58. https://doi.org/10.1051/cocv/2018036.
- [8] R.D.A. Capistrano-Filho, M.M.D.S. Gomes, Well-posedness and Controllability of Kawahara Equation in Weighted Sobolev Spaces, Nonlinear Anal. 207 (2021), 112267. https://doi.org/10.1016/j.na.2021.112267.
- [9] L.C. Evans, Partial Differential Equations, American Mathematical Society, 2010.
- [10] J. Frauendiener, C. Klein, U. Muhammad, N. Stoilov, Numerical Study of Davey–Stewartson I Systems, Stud. Appl. Math. 149 (2022), 76–94. https://doi.org/10.1111/sapm.12491.
- [11] G.E. Karniadakis, S. Sherwin, Spectral/hp Element Methods for Computational Fluid Dynamics, Oxford University Press, 2013.
- [12] T. Kato, Low Regularity Well-Posedness for the Periodic Kawahara Equation, Differ. Integral Equ. 25 (2012), 1011–1036. https://doi.org/10.57262/die/1356012249.
- [13] R.I. McLachlan, G.R.W. Quispel, Splitting Methods, Acta Numer. 11 (2002), 341–434. https://doi.org/10.1017/ s0962492902000053.
- [14] D. Russell, B. Zhang, Exact Controllability and Stabilizability of the Korteweg-De Vries Equation, Trans. Am. Math. Soc. 348 (1996), 3643–3672. https://doi.org/10.1090/s0002-9947-96-01672-8.
- [15] P.J. Olver, Applications of Lie Groups to Differential Equations, Springer, New York, 2010. https://doi.org/10.1007/978-1-4612-4350-2.
- [16] S.S. Sabo, U.M. Dauda, S. Babuba, A.I. Bakari, On Nonlinear Biharmonic Dispersive Wave Equations, FUDMA J. Sci. 9 (2025), 87–100. https://doi.org/10.33003/fjs-2025-0901-2925.
- [17] T. Saanouni, R. Ghanmi, A Note on the Inhomogeneous Fourth-Order Schrödinger Equation, J. Pseudo-Differ. Oper. Appl. 13 (2022), 56. https://doi.org/10.1007/s11868-022-00489-0.
- [18] W.A. Strauss, Nonlinear Wave Equations, American Mathematical Society, 1990.
- [19] T. Tao, Nonlinear Dispersive Equations: Local and Global Analysis, American Mathematical Society, 2006.

- [20] L. N. Trefethen, Spectral Methods in MATLAB, SIAM, 2000.
- [21] B. Zhang, X. Zhao, Control and Stabilization of the Kawahara Equation on a Periodic Domain, Commun. Inf. Syst. 12 (2012), 77–96. https://doi.org/10.4310/cis.2012.v12.n1.a4.
- [22] X. Zhao, B. Zhang, Global Controllability and Stabilizability of Kawahara Equation on a Periodic Domain, Math. Control. Relat. Fields 5 (2015), 335–358. https://doi.org/10.3934/mcrf.2015.5.335.
- [23] X.Z. Xiangqing Zhao, M.B. Meng Bai, Control and Stabilization of High-Order Kdv Equation Posed on the Periodic Domain, J. Partial. Differ. Equ. 31 (2018), 29–46. https://doi.org/10.4208/jpde.v31.n1.3.